KNOCK CONTROL FOR DIESEL DUAL FUEL ENGINE

PATIN PONGKACHA

A THESIS SUBMITTED IN PARTIAL FULFILLMENT

OF THE REQUIREMENT FOR THE DEGREE OF

MASTER OF ENGINEERING IN AUTOMOTIVE ENGINEERING

INTERNATIONAL COLLEGE

KING MONGKUT'S INSTITUTE OF TECHNOLOGY LADKRABANG

2012

KMITL-2011-IC-M-004-013

Thesis Title	Knock Control For Diesel Dual Fuel Engine
Student	Mr. Patin Pongkacha
Student ID.	50061909
Degree	Master of Engineering
Program	Automotive Engineering (International Program)
Year	2012
Thesis Advisor	Assoc. Prof. Dr. Pitikhate Sooraksa
Thesis Co-Advisor	Asst. Prof. Dr. Chinda Charoenphonphanich
Thesis Co-Advisor	Assoc. Prof. Masaki Yamakita
Thesis Co-Advisor	Dr. Teera Phatrapornnant

ABSTRACT

Diesel Dual Fuel (DDF) is a promising approach in reduction of diesel fuel consumption for diesel vehicles; however, knock phenomenon is a major serious problem in DDF engine because of the difference in compression ignition characteristics of gaseous fuel and diesel fuel. This thesis presents the study of knock control for DDF engine, which can be used as an engine-fault monitoring, on a four cylinders DDF engine fueled with diesel and natural gas. This work begins with developing a knock detection strategy. Discrete wavelet transform (DWT) with lifting scheme algorithm is employed to process and filter unwanted signal components. Mutually, statistical Chi-square method is also applied in order to discriminate knock from noise signals. Simulation and experimental results show that the proposed method can effectively sense the knock features. Furthermore, the proposed knock detection and control algorithm is also proved on a small single-cylinder and four-cylinder diesel engines as the realistic case studies. Conceptually, the knock control strategy based on the ignition retard control of spark ignition (SI) engine is applied as

knock table update method to compensate the amount of alternative fuel supplements to the DDF engine; therefore, elimination of DDF knock is due to its intensity controllable.

ACKNOWLEDGMENTS

I would especially like to thank Assoc. Prof. Dr. Pitikhate Sooraksa for being the best advisor not only for instructing me in academic area but also encouraging me so that I can pass through the difficult period. This dissertation would not have been possible without him.

I appreciate valuable comments and advices from Dr. Teera Phatrapornnant, Assoc. Prof. Masaki Yamakita and Asst. Prof. Dr. Chinda Charoenphonphanich with kindness. I really grateful to Tokyo Institute of Technology (Tokyo Tech) and my work place, National Science and Technology Development Agency (NSTDA) for giving me the great opportunity to enhance my knowledge, experiences and also provided the scholarship.

I would like to say many thanks to my friends at Embedded System Technology Laboratory of NECTEC whose participated and shared their expertise in this thesis: Mr. Jaturawit Janpaiboon, Mr. Suradech Doungpummet, Mr. Montri Chatpoj and Mr. Paniti Sira-Uksorn for advising and cheering me up during the hard days. I wish to convey my sincere thanks to Ms. Thanthita Sethphakchaiyakorn who always support me. A very special thanks to Mr. Paniti Pumviset for giving me his lovely car to use as a test car in my experiments.

Last but not least, I thank my family for their continuous love and care.

Patin Pongkacha

TABLE OF CONTENTS

TABLE OF CONTENTS (CONT.)

TABLE OF CONTENTS (CONT.)

LIST OF TABLES

LIST OF FIGURES

LIST OF FIGURES (CONT.)

LIST OF FIGURES (CONT.)

CHAPTER 1

INTRODUCTION

1.1 Background and Problem

The compression ignition (CI) engine (known as the diesel engine) is the main power-train in transportation sector, while the diesel price has risen continuously. Regarding to the raise of diesel price, the transportation sector turn their interested to alternative fuels, which is cheaper and locally available. In Thailand, the available alternative fuels for use instead of diesel are: biodiesel as the B5 (5% mix with normal diesel), compressed natural gas (CNG) and liquefied petroleum gas (LPG). However, the most recommended by the government and cheapest is CNG. The CNG can be used in diesel engine by installs the gas injection components to modify to be DDF system. But the important problem of DDF system is the knock. Too much knock can give severe damage to the engine, and the rate of using gas instead of diesel in DDF engine is also limited by knock [17].

Knock in DDF engine is due to the different compression ignition characteristics between diesel fuel and gaseous fuel. It does not only depends on too much quantity of gaseous fuel in the combustion chamber, but also on other factors such as engine speed, engine load, inlet gas/air mixture temperature and so on, which are the uncontrollably factors when the engine operates under real-world operating conditions. Those circumstances limit the amount of gaseous fuel to replace diesel fuel. An idea of knock control in this work, bases on the ignition retard control in spark SI engine when spark knock onset. To control a DDF engine, knock detection is one of a crucial process in order to determine the appropriate amount of alternative fuels supplied to the engine.

1.2 Literature Review

There are many works using in-cylinder pressure to detect knock by measuring the pressure resonances [3, 4, 8] and these methods gave accurate results. However, knock detection using in-cylinder pressure is normally used in laboratory because of its cost and durability of this sensor type. In car production, they are commonly used acceleration sensors - as knock sensors - mounted on the engine housing to gauge the engine vibrations at its mounting location. In this case, signal-to-noise ratio (SNR) of the measured signals are typically low because it is interfered by the engine background noises, such as intake valve closing (IVC), exhaust valve closing (EVC) and other vibrations due to mechanic events [3, 16]. The classical method of knock detection is to estimate the energy of the vibration signal filtered by the band-pass filter and compare it to a certain threshold [2, 3, 10, 16]. However, it is complicated to distinguish the engine knock accurately from such a very low SNR of vibration signal.

Wavelet transform has appeared in the context of the time-frequency representation (TFR). Many researchers have applied the wavelet transform to vibration signals, e.g. false analysis and diagnosis of rotating machinery [1, 11, 15, 18]. Some researchers have been done on transient detection by applying both the TFR and statistic methods [15, 18]. Zhua et al. [18] presented a transient detection method that combines continuous wavelet transform (CWT) and Kolmogonov-Smirnov (K-S) test for machine fault diagnosis. From the existing applications of the wavelet transform, it potentially applies for detecting knock signal due to its transient features of the vibration signal.

However, CWT requires high computational system which is difficult to implement on a vehicle. A fast computational wavelet method is then introduced by J. Fiolka [8], for detecting knock. It is called wavelet base knock detection (WBKD). WBKD is based on joint time-frequency analysis of the pressure signal, and can suppress the noise in the wavelet domain in order to detect knock efficiently.

Moreover, using discrete wavelet transform with lifting scheme algorithm has low computational complexity.

1.3 Objectives

The goal of this research is to develop the knock control for DDF engines. The concept is using the information from an additional knock sensor to compensate gas injection to the inlet manifold; besides, the DDF knock could be eliminated on account of the optimum gas injection duration.

In order to achieve the overall goal, the objectives are concluded below:

1. Design the knock detection algorithm for DDF engines.

2. Design the knock control system corresponding to the first step above.

3. The designed knock control system can eliminate the knock phenomena for a traditional DDF system.

1.4 Scopes

Regarding to the several mechanical parts and various operations of the DDF engines, the scopes of this research are explained below:

1. The DDF engine operations as no adjustment for amount of diesel injection.

2. The input signals to be used in knock evaluation are those from knock sensor, crank position, engine speed, throttle position and the gas injection.

3. Only one channel and one type of knock sensor will be used in the implementation and not focus on the location of knock sensor mounts to the engine.

4. The experiment focuses on comparison between the DDF system that enables the knock control system and disabled one.

1.5 Research Methodology

This research begins with developing a knock detection strategy. In order to reach this purpose, the various knock detection techniques will be selected from literature reviews and comparison on the simulation studies. When the designed knock detection technique performs well in the simulation results, this algorithm allows to be applied for a real engine experiment. Since the proposed method is effective for knock detection in the real system, the next step is to develop a knock control strategy. After that, the experiment of knock control will be processed until the results have been approved. Finally, summarization and the thesis writing will be performed. The diagram of research methodology is showed in Figure 1.1.

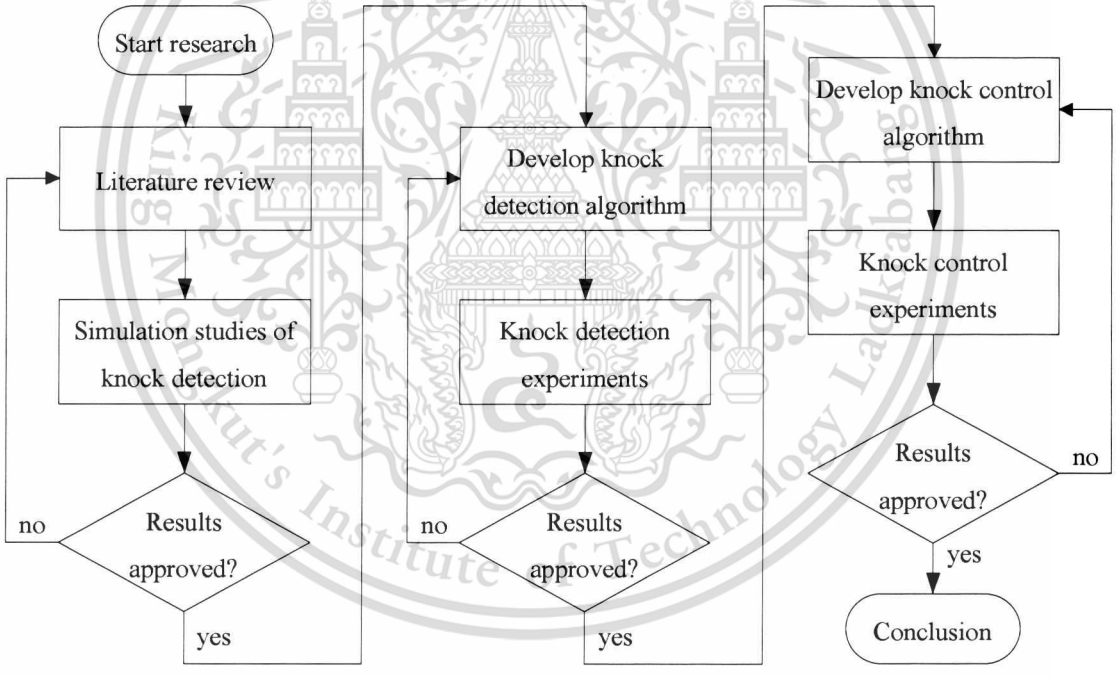

Figure 1.1 Research methodology diagram

1.6 Research Overview

This research is divided into five chapters. Chapter 1 is the current chapter, which introduces the research topic and summarizes the details on the literature

reviewed earlier before commencing on the adaptation stage. In the last of this chapter explains on the objectives, scopes and methodology of the research.

The following Chapter 2 will focus on the theoretical explanation of the method used in the computational frequency transformation such as the Fourier transform and short time Fourier transform, which are discussed further in this chapter as well as the introduction to the wavelet transform. The comparison on three types of transformation is discussed in the end of the chapter.

Next, in Chapter 3 will explain about the combustion knock and the types of knock in DDF engine. Besides that, the essential methods such as: wavelet-based knock detection, the combination with Chi-square statistical threshold and the knock control strategy are explained.

After the proposed methods are explained in Chapter 3, all the simulation and realistic engine tests results will be showed and discussed in Chapter 4. Moreover, this chapter will give all the relevant calculations and the signal conditions that are required for the knock detection and control strategy.

Finally, the conclusion will be made in Chapter 5 by concluding the overall results obtained as well as the knowledge learned from this research.

CHAPTER 2

BACKGROUND THEORY

Since wavelet and wavelet transform are the modern approach for signal or image analysis, the information of time and frequency can be obtained. It is well known, wavelet transform was developed to solve the problems that cannot do by Fourier transform (FT) and short time Fourier transform (STFT). Because wavelet transform is similar to both FT and STFT, this chapter mentions FT and STFT for background to understand wavelet transform.

2.1 Fourier Transform

FT is a signal transformation methodology to transform the signal from time domain to frequency domain. It is based on the principle that any wave, including by the summation of various frequencies of sinusoidal.

$$X(f) = \int_{-\infty}^{\infty} x(t) \cdot e^{-2j\pi ft} dt \tag{2.1}$$

$$x(t) = \int_{-\infty}^{\infty} X(f) \cdot e^{2j\pi ft} df \tag{2.2}$$

Equation (2.1) is the transformation equation to make FT of a signal. This equation shows that if the signal has any frequency which is the same as sinusoidal frequency f, the result will be showed as the peak amplitude in the frequency domain of FT. Equation (2.2) is the inverse transformation equation, which used to reverse FT of the signal back to the time domain signal.

FT can represent the frequency components of the signal but it does not have the detail of what time does the frequency occur, see Figure 2.1, Figure 2.2, Figure 2.3 and Figure 2.4.

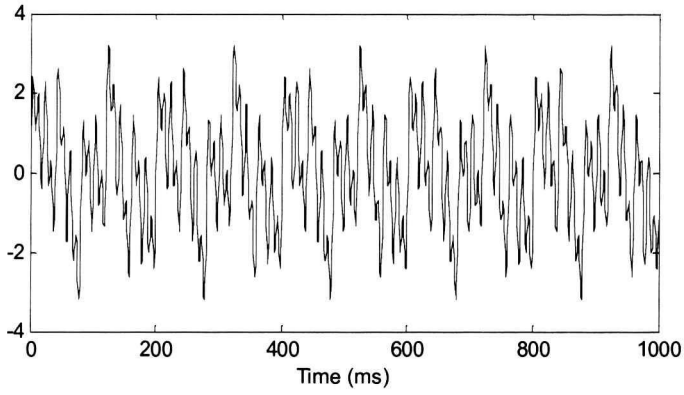

Figure 2.1 Stationary signal has frequency of 100, 50, 25 and 10 Hz.

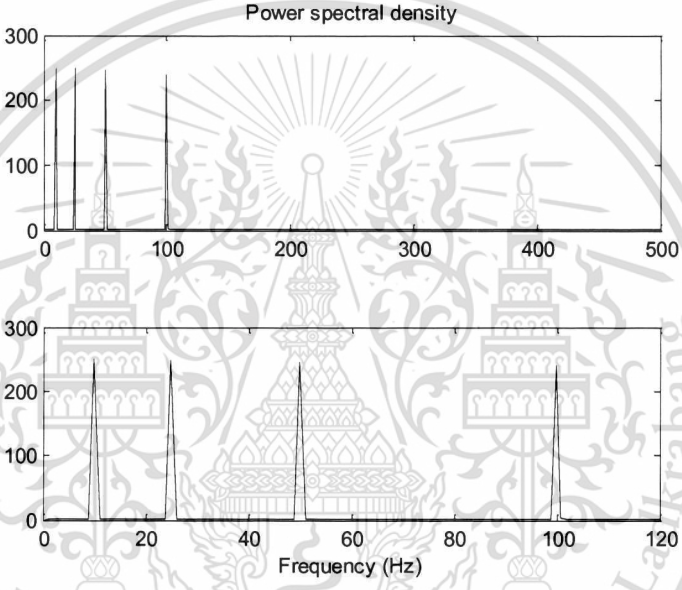

Figure 2.2 FT of the signal in Figure 2.1

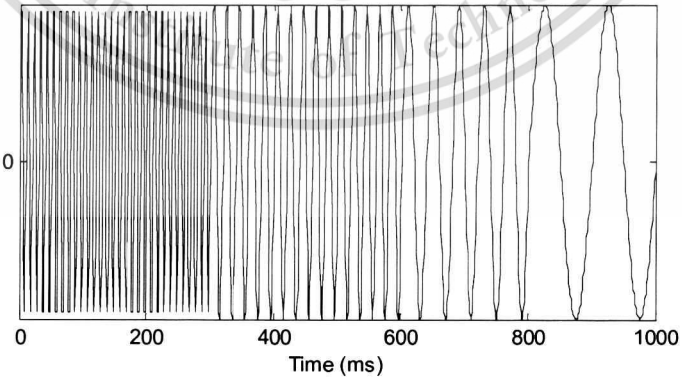

Figure 2.3 Non-stationary signal has frequency of 100, 50, 25 and 10 Hz.

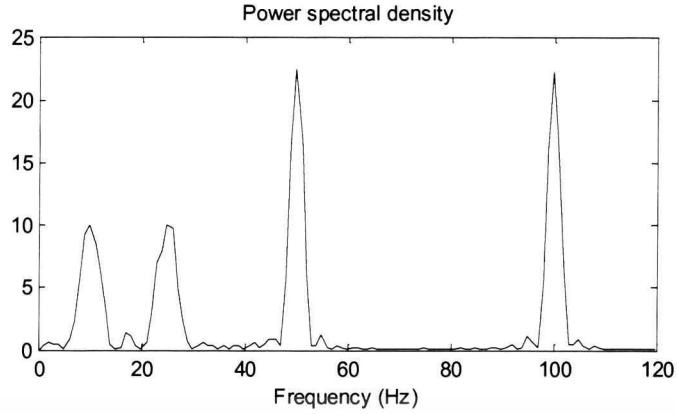

Figure 2.4 FT of the signal in Figure 2.3

Figure 2.1 shows a signal that the frequency does not change with time. When all frequency components contain in any time of the signal, it means as the stationary signal. Both of the signals shown in Figure 2.1 and Figure 2.3 have the same frequency components which appear in different shape although FT of those signals show in Figure 2.2 and Figure 2.4 are also the same (only the peak amplitude, but excluding any minor detail of FT). As above mentioned, FT can represent only the frequency, but it does not have detail about the time. FT can identify what frequency contains in the signal while it cannot know what time does that frequency occurring. Consequently, FT does not appropriate to analyze the signal that the time detailing is required, such as the signal in Figure 2.3. However, improving of analysis by using STFT can obtain both frequency and time detailing.

2.2 Shot Time Fourier Transform

STFT is a signal transformation which transforms the signal from time domain to the frequency domain corresponding to the short time interval. The concept is the same as FT which appropriates for stationary signal. In order to calculate STFT, the non-stationary signal will be divided into small intervals, which can be defined as the stationary signals. Finally, each small interval signal can be analyzed by using FT.

The calculation of dividing signal is achieved by using the window as a time selection tool. The process begins with apply the window at the start of the signal and then calculates the windowed signal using FT. After that, moves the window to

select the next part of signal for calculation and repeat until the end of signal. Translation of the window can achieve the time information, whereas FT calculation can achieve the frequency information.

Signal transformation using STFT shows in Equation (2.3).

$$STFT_x^{(\omega)}(t', f) = \int_t \left[x(t) \cdot \omega * (t - t')\right] \cdot e^{-j2\pi ft} dt \tag{2.3}$$

Following figures show the signal and its STFT using different size of windows. In this example, a window function is the Gaussian function shown in Equation (2.4).

$$w(t) = \exp\left(\frac{-a * t^2}{2}\right) \tag{2.4}$$

where, a is the window length and t is the time.

Each transformation of STFT uses a fix window length, so the results of the overall signal are in the same resolution of both time and frequency (even if the resolution is accurate or not).

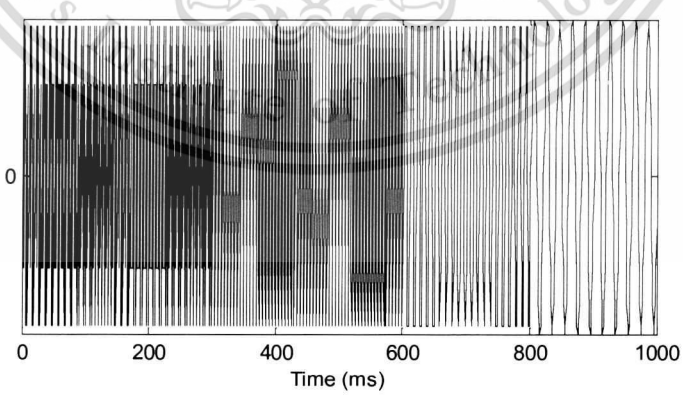

Figure 2.5 Signal has the frequency of 300, 200, 100 and 50 Hz, respectively.

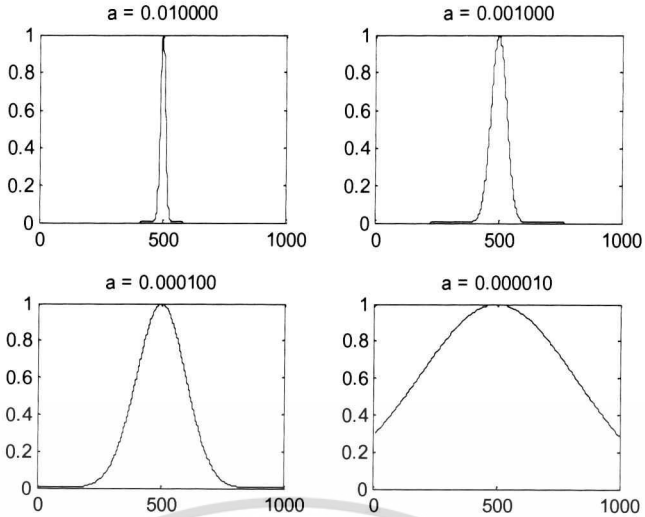

Figure 2.6 Window length a=0.01, 0.001, 0.0001 and 0.00001

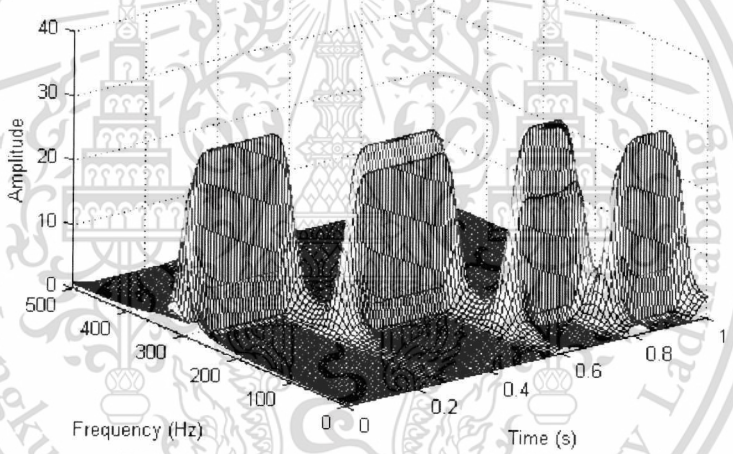

Figure 2.7 STFT of the signal in Figure 2.5 by using a=0.01

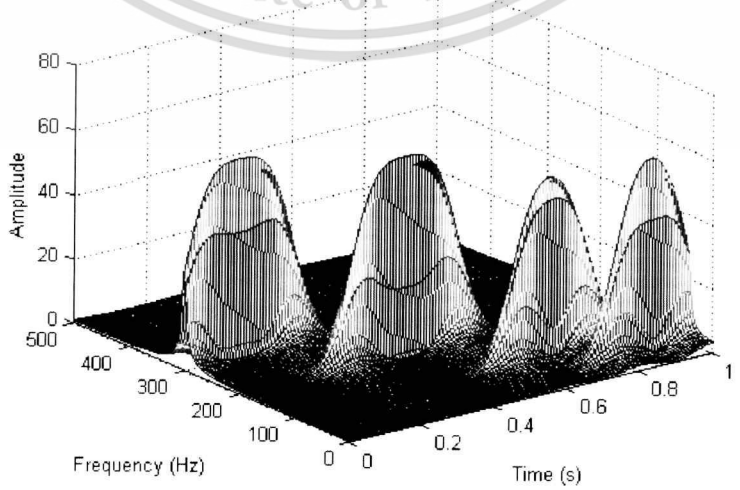

Figure 2.8 STFT of the signal in Figure 2.5 by using a=0.001

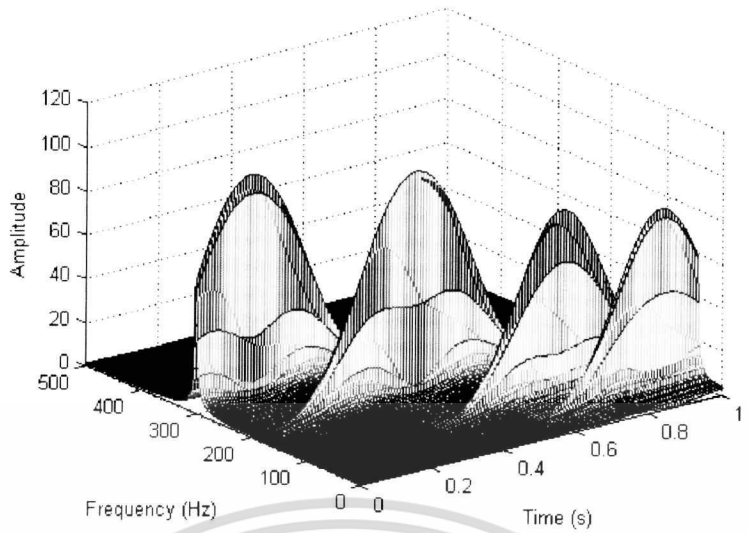

Figure 2.9 STFT of the signal in Figure 2.5 by using a=0.0001

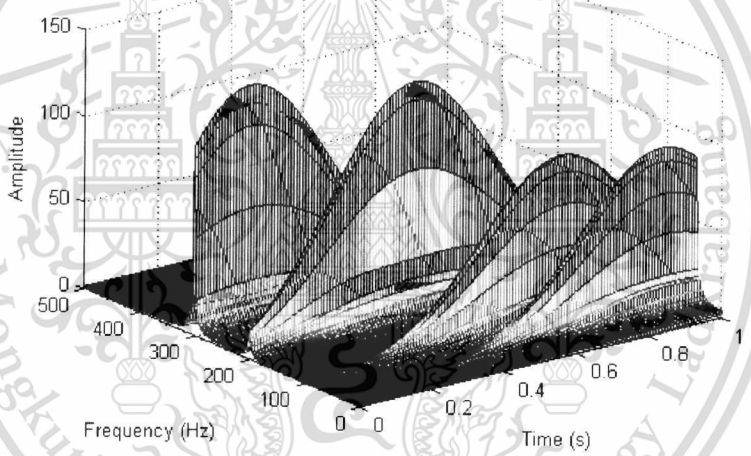

Figure 2.10 STFT of the signal in Figure 2.5 by using a=0.00001

When use the narrow window as shown in Figure 2.7 and Figure 2.8, the good time resolution is represented as the determination of time division is obviously. However, the frequency resolution is poor since each time duration has a wide frequency range and cannot clearly identify what the frequency is. When use wider window as shown in Figure 2.9 and Figure 2.10, the time resolution is reduced as the time detailing is more unclear while the frequency resolution is increased. The disadvantages of STFT are concluded as follows:

1. The narrower the window, the better the time resolution, but the poorer the frequency resolution.

2. The wider the window, the poorer the time resolution, but the better the frequency resolution, and cannot determine the non-stationary signal as the stationary signal.

As above mentioned, STFT has the disadvantages of resolution, so it leads to the modern analysis which is wavelet transform (WT).

2.3 Wavelet Transform

As mentioned earlier in the signal analysis, FT can represent only the frequency without the time information, whereas STFT can represent both frequency and time. However, the disadvantages of STFT are about the resolutions: if obtains the good time resolution then the frequency resolution will be low, but if obtains the good frequency resolution then the time resolution will be low. To overcome these weaknesses, the modern signal analysis called multi-resolution analysis (MRA) is used to analyze the signal. With respect to using MRA, each interval is represented in the different resolution. The new approach is different from STFT which analyzes a signal by using only a single resolution of time and frequency for all frequency components in the signal, even if the resolution is accurate or not. The resolutions obtained by MRA are described below:

1. In the high frequency range of the signal, MRA gives a good time resolution but poor frequency resolution.

2. In the low frequency range of the signal, MRA gives a poor time resolution but good frequency resolution.

The difference in frequency as mentioned above has the benefit for any low frequency signal that has the short range of high frequency. The common signal in the real world such as in Figure 2.11 also has the characteristic as the mentioned.

Figure 2.11 Signal that has a short range of high frequency

2.3.1 Definition of Wavelet and Mother Wavelet

Wavelet is a small wave that has the limits of length and energy. It is used as a tool to analyze those of the signals that: the frequency change with time (time-varying signal), the frequency change immediately (transient signal) and non-periodic (non-stationary signal). Wavelet function performs as the window function and the exponential function in STFT.

Mother wavelet is an ideal wavelet that is used to generate the other wavelets by such as compression or expansion of mother wavelet. There are many models of the mother wavelets, for instance, Daubechies, Harr, Symiets, Coiflets, Moriet, Mexican hat and so on. Moreover, the mother wavelets are also categorized into the family. Figure 2.12 and Figure 2.13 show Coiflets family and Daubechies family, respectively.

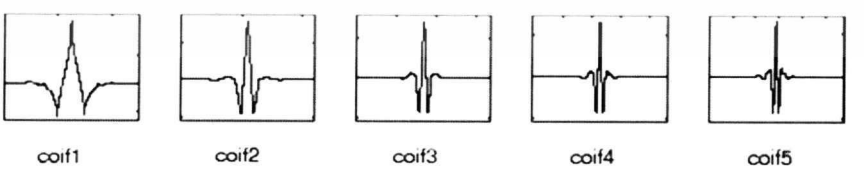

Figure 2.12 Example of Coiflets wavelet family

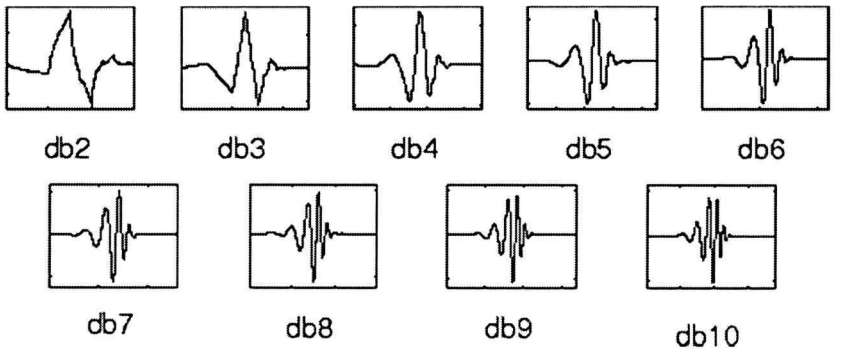

Figure 2.13 Example of Daubechies wavelet family

2.3.2 Definition of Wavelet Transform and Multi-Resolution

Wavelet transform is a signal that was transformed into the domain of frequency and time. The process is to calculate the original time domain signal by using transformation equation with a suitable wavelet. After that, the result, wavelet transform of the original signal will be obtained. This wavelet transform can represent the frequency with its corresponding time contained in the signal.

Wavelet transform is similar to both FT and STFT. The comparison between 3 techniques is shown in Table 2.1

Table 2.1 Comparison between FT, STFT and WT

FT	STFT	WT
Use FT equation	Use STFT equation	Use WT equation
Use exponential function $e^{-2j\pi ft}$ as basis function.	Use exponential function same as FT, and also use window function $\omega*(t-t')$	Use wavelet $\psi^*_{\tau,s}(t)$ as basis function.
The concept is any wave consists of the combination of the various sinusoidal frequencies.	The concept is the same as FT, but the difference is to divide any signal into small intervals before the calculation to get time and frequency information of the signal.	The concept is to substitute any wave with the summation of the small waves that have the limits of length and energy, so it can obtains both time and frequency information of the signal.
The transformation result is a function of frequency, so any frequency that contains in any wave will be represented.	The transformation result is a function of frequency and time, so any frequency at any time will be represented. But the limitation is the resolution of frequency and time will be all the same in any frequency of the signal.	The transformation result is a function of frequency and time, so any frequency at any time will be represented. Moreover, the resolution of frequency and time will be changed respecting to the frequency contain in the signal.
Not MRA	Not MRA	MRA

2.3.3 Discrete Wavelet Transform

Wavelet transform is known as an efficient tool for time-frequency analysis of the signals. The analysis involves the decomposition of the signals on a set of basis function. The analyzing function is $\psi_{a,b}(t)$, which is a scaled and shifted version of

mother wavelet $\psi(t)$. The CWT of $f(t)$ is defined as summation over all time of the signal multiplied by the analyzing function, given by:

$$CWT(a,b) = \int_{-\infty}^{\infty} f(t) \cdot \psi_{a,b}^{*}(t) dt \tag{2.5}$$

where

$$\psi_{a,b}(t) = \frac{1}{\sqrt{a}} \psi\left(\frac{t-b}{a}\right), \quad a \in \Re^{+}, b \in \Re \tag{2.6}$$

In Equation (2.6), the parameter a represents the scale index associated with frequency ($|a| > 1$ dilates the wavelet and $|a| < 1$ compresses the wavelet). The factor $1/\sqrt{a}$ is for energy normalization across the different scales. The parameter b is the translation factor (time shifting). To overcome the redundancy of CWT, the DWT is preferred by sampling a continuous set of a and b to $a = 2^{-j}$ and $b = k \cdot 2^{-j}$. Substitution in Equation (2.5), yields:

$$DWT(j,k) = \int_{-\infty}^{\infty} f(t) \cdot \psi_{j,k}^{*}(t) dt \tag{2.7}$$

where

$$\psi_{j,k}(t) = \sqrt{2^{j}} \psi(2^{j} t - k), \quad j,k \in Z \tag{2.8}$$

The DWT can be performed by using multi-resolution algorithm developed by Mallet [12]. The analyzed signal $f(t)$ as input is processed through scaling function (low-pass filter) and wavelet function (high-pass filter) and then downsample to obtain the coefficients. The approximation coefficients are obtained by scaling function, whereas the detail coefficients can be obtained by wavelet function. The approximations become the input for the next level of decomposition, and the process is iterated until either the required resolution or complete decomposition has been achieved. Having two types of coefficients, the analyzed signal $f(t)$ can be written as:

$$f(t)=\sum_{k} c_{j_0,k}\varphi_{j_0,k}(t)+\sum_{k}\sum_{j=j_0}^{J} d_{j,k}\psi_{j,k}(t) \tag{2.9}$$

where

$c_{j_0,k}$ is approximation coefficients

$\varphi_{j_0,k}(t)$ is scaling function, and

$d_{j,k}$ is detail coefficients

In Equation (2.9), j represents the decomposition level and k is the coefficient index. In practice, the indexes j_0, j and k are determined by the sampling rate and by the size of the feature of interests in the signal $f(t)$.

CHAPTER 3

KNOCK DETECTION AND CONTROL IN DIESEL DUAL FUEL ENGINE

3.1 Combustion Knock in Diesel Dual Fuel Engine [14]

Figure 3.1 shows typical pressure crank angle diagrams of dual fuel operation. The gas-injected dual fuel engine has combustion characteristics which lie between those of CI and SI engines. It involves evolution of two stages of ignition and combustion processes resulting in about two types of knock. The combustion processes in dual fuel pilot injection system have been identified as taking place in five stages as shown in Figure 3.1. The phases are: the pilot ignition delay (AB), pilot premixed combustion (BC), primary fuel delay period (CD), rapid combustion of primary fuel (DE) and the diffusion combustion stage (EF).

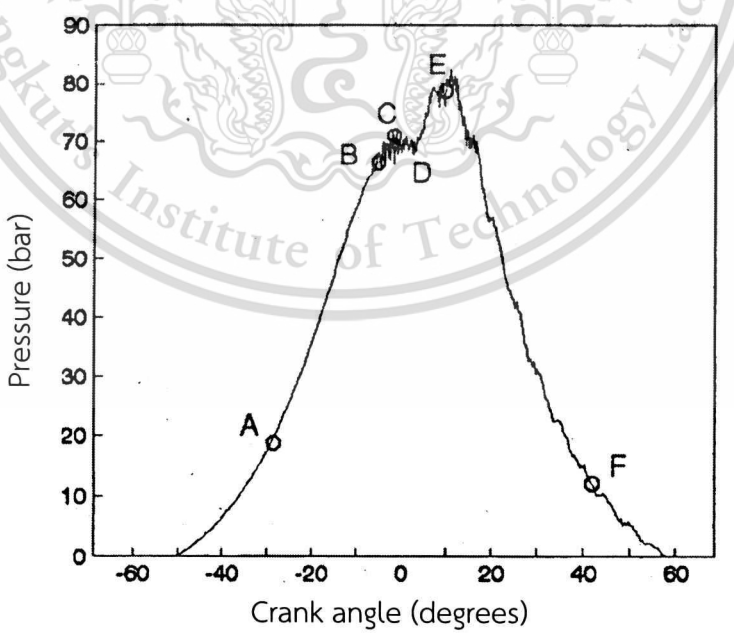

Figure 3.1 Dual fuel pilot injection pressure-crank angle diagram [14]

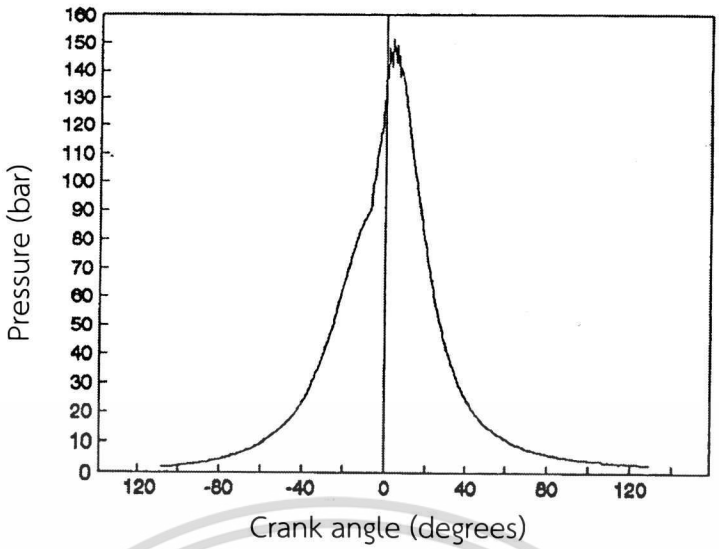

Figure 3.2 Pressure-crank angle diagram of diesel fuel operation [14]

3.1.1 Diesel Knock in Diesel Dual Fuel Engine [14]

Diesel engines are generally noisy and knock occur at all operating conditions especially when the engine is cold. The knock referred to in this scheme of work is an objectionable knock characterized by high pitch metallic sound. Figure 3.2 shows pure diesel fuel operation and can be compared with Figure 3.1 showing dual fuel operation. The ripples in Figure 3.1 are absent in Figure 3.2, and are a result of combustion knock. Dual fuel operation showed longer ignition delay as a comparison between Figure 3.1 and Figure 3.2. Since the fuel metering system continues to inject fuel throughout the delay period, it was then thought that in dual fuel systems, large quantities of premixed fuel would be involved when ignition eventually occurs. In an oxygen (O_2) depleted environment, it was thought that only a small quantity of pilot fuel reacts with O_2 before auto-ignition of the mixture. The degree of knock in this phase was noted to depend on the ratio of the alternative fuel (natural gas) to the pilot fuel. This ratio is seen to depend on the load and speed of operation. It is a known fact that increases in speed increases the ignition delay when running on pure diesel fuel; hence the quantity of premixed pilot fuel that takes part in combustion increases.

3.1.2 Spark Knock in Diesel Dual Fuel Engine [14]

Knocking combustion in SI engine has been identified to be due to auto-ignition of the end gas. When auto-ignition occurs during normal combustion, the phenomenon is called “spark knock”. When knock occurs, high frequency pressure fluctuations are observed whose amplitude decays with time. These pressure fluctuations produce the sharp metallic noise called knock. In a dual fuel engine, ignition occurs at different points in the chamber after the delay period unlike the single point ignition process of an SI engine. It involves two stages of ignition and combustion processes. The first combustion is due to auto-ignition of the pilot fuel, and then there is a finite time interval, as shown in Figure 3.1 (CD), for the second combustion to commence. This finite time is sufficient for heat transfer to the end gas to take place which increases the end gas pressure, temperature and reaction rate. These processes are influenced by the combustion chamber design and the level of turbulence in the cylinder. The dual fuel operation is characterized by pressure fluctuations especially at low load levels where the delay period is seen to be longer. This fluctuation is reduced at high load and temperature due perhaps to the reduction in delay period and improved combustion at these operating conditions. The auto-ignition of a gaseous fuel-air mixture occurs when the energy released by the reaction as heat is larger than the heat lost to the surroundings. The temperature of the mixture therefore increases, which in turn increases the rates of reaction until self-ignition temperature (SIT) is reached. The degree of spark knock in dual fuel engine also depends on the time interval between the first and second ignition. It is seen to decrease with increased load and combustion temperature. This is contrary to the knock in SI engines which increases with increased combustion temperature. The reason for this perhaps is the reduced delay period, a result of high combustion temperature.

3.1.3 Effect of Alternate Fuel on Diesel Dual Fuel Engine

From the treatment conditions of knock onset in DDF engine, the result is difference when using each type of alternative fuel, LPG and CNG. Using LPG is easier for the spark knock onset because the SIT of LPG is lower than CNG. In DDF engine, the spark knock occurs because of the self-ignition of the gaseous fuel-air mixture during the compression stroke when the SIT of the premixing gaseous fuel is reached. Since CNG has high SIT, the spark knock of using CNG will occur when the combustion chamber reaches the high temperature. Besides, it can extremely reduce the durability of the engine. Generally, the diesel knock will occur before the spark knock onset in dual fuel operation. Moreover, too much diesel knock will causes the spark knock to commence. The reason is due to the long ignition delay that takes place during diesel knock allowing the heat transfer to the end gas.

3.2 Wavelet-Based Knock Detection

In the real world, noise is one of the major obstacles for detecting engine knock. Some noise components can be modeled as Gaussian noise and there are some transient components having the same frequency as knock, such as IVC and EVC. Fortunately, these transients do not appear at the same time of the knock period.

In order to detect knock signal in noisy environment, wavelet transform is one of the promising methods which has noise suppression capability [8]. On the other hand, Chi-square, which is a statistical method, can be employed to discriminate different transient signals [18]. We then propose the combined method, WBKD with statistical threshold using Chi-square statistics, to detect engine knocking. The proposed knock detection diagram is showed in Figure 3.3.

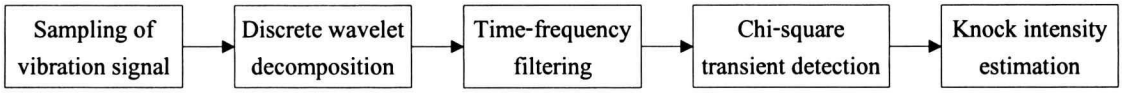

Figure 3.3 Diagram of the proposed knock detection method

3.2.1 A Lifting Scheme Version of Daubechies D8 Transform

Any two-channel filter bank can be factored into a finite number of lifting steps [5]. The lifting consists of three steps: split, predict and update (See Figure 3.4).

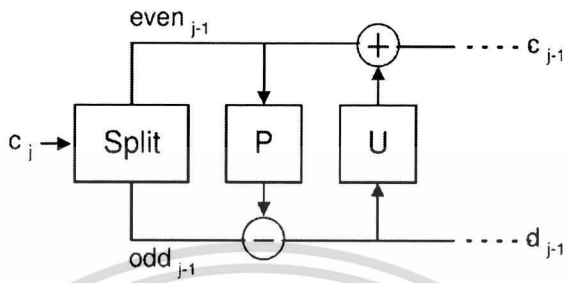

Figure 3.4 The one-level forward wavelet transforms using lifting scheme

The algorithm starts with a split step, which divides the input data into odd and even elements. The predict step subtracts a filtered version of the even input to the odd input.

$$d_{j-1} = odd_{j-1} - P(even_{j-1}) \tag{3.1}$$

The update step adds a filtered version of the lifting output to the even input.

$$c_{j-1} = even_{j-1} + U(d_{j-1}) \tag{3.2}$$

MATLAB function, liftwave('db8') returns a structure of the lifting scheme associated with the Daubechies D8 wavelet. This specific structure is showed in Table 3.1

Table 3.1 Corresponding lifting scheme of db8 wavelet

d	-5.74964161417150	0
p	-0.0522692017330962, 0.168817243656942	1
d	14.5428210043619, -7.40210683661006	-1
p	-0.0324020739512596, 0.0609092564633227	3
d	5.81871649072316, -2.75569878810593	-3
p	0.945295268115791, 0.242021684432458	5
d	0.000188840253682300, -0.00180381587421570	-3
p	-0.952613831895766, -0.224138162416755	5
d	1.04974329437902, -0.246991733177599, 0.0271973973533717	-5
	3.54936225413563, 0.281740754648197	

The structure in Table 3.1 is 10×3 cell array. The 9 first rows of the array are elementary lifting steps. The last row gives the normalization of lifting scheme. The columns in elementary lifting steps, from left to right, are type, coefficient and max degree, respectively. Where, type is p (primal) or d (dual), coefficients is a vector C of real numbers defining the coefficients of a Laurent polynomial P, and max degree is the highest degree d of the monomials of P. The Laurent polynomial P is described below.

$$P(z) = C_1 z^{d} + C_2 z^{d-1} + \ldots + C_m z^{d-m+1} \tag{3.3}$$

Hence, it corresponds to the following implementation of the one-level forward transform:

$$d_l^{(1)} = x_{2l+1} - 5.74964161417150 x_{2l}$$

$$c_l^{(1)} = x_{2l} - 0.0522692017330962 d_{l+1}^{(1)} + 0.168817243656942 d_l^{(1)}$$

$$d_l^{(2)} = d_l^{(1)} + 14.5428210043619 c_{l-1}^{(1)} - 7.40210683661006 c_{l-2}^{(1)}$$

$$c_l^{(2)} = c_l^{(1)} - 0.0324020739512596 d_{l+3}^{(2)} + 0.0609092564633227 d_{l+2}^{(2)}$$

$$d_l^{(3)} = d_l^{(2)} + 5.81871649072316 c_{l-3}^{(2)} - 2.75569878810593 c_{l-4}^{(2)}$$

$$c_l^{(3)} = c_l^{(2)} + 0.945295268115791 d_{l+5}^{(3)} + 0.242021684432458 d_{l+4}^{(3)}$$

$$d_l^{(4)} = d_l^{(3)} + 0.000188840253682300 c_{l-3}^{(3)} - 0.00180381587421570 c_{l-4}^{(3)}$$

$$c_l^{(4)} = c_l^{(3)} - 0.952613831895766 d_{l+5}^{(4)} - 0.224138162416755 d_{l+4}^{(4)}$$

$$d_l^{(5)} = d_l^{(4)} + 1.04974329437902 c_{l-5}^{4} - 0.246991733177599 c_{l-6}^{4} + 0.0271973973533717 c_{l-7}^{4}$$

$$c_l = 3.54936225413563 c_l^{(4)}$$

$$d_l = 0.281740754648197 d_l^{(5)}$$

3.2.2 Time-Frequency Filtering

Time-frequency filtering is a method of noise suppression within the wavelet domain by zero padding the coefficients that contain in out-of-boundary time-scale plane. See Figure 3.5, the coefficients (e.g. $d_{j+2,1}$, $d_{j+1,1}$, $d_{j,1}$, $d_{j,2}$ and so on) are set to zero shown in the dark color. Thus, the important features of the signal can be represented by a small set of the extracted coefficients.

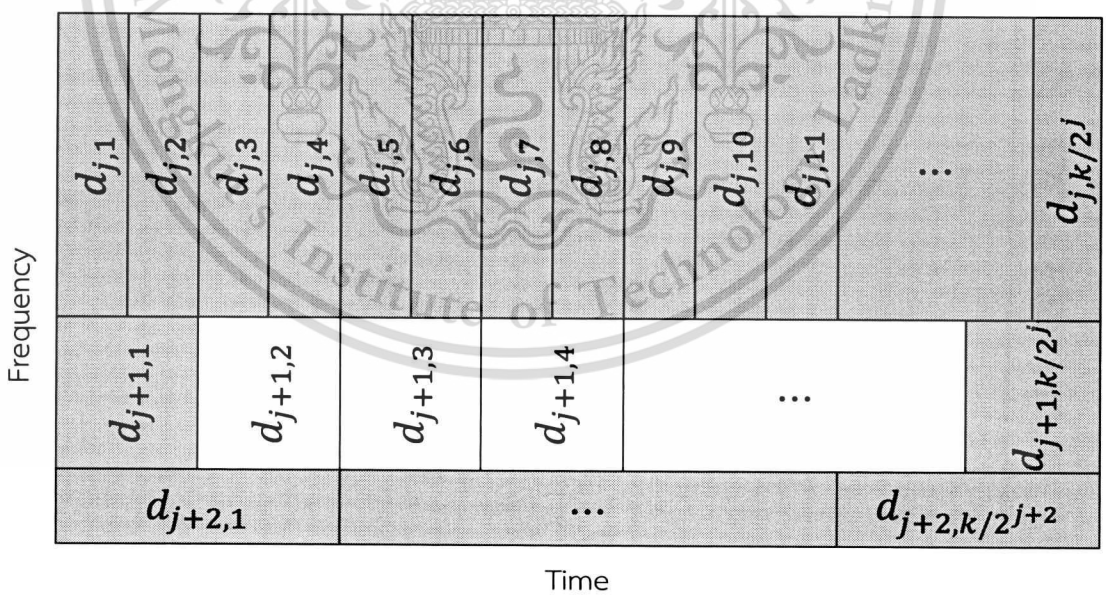

Figure 3.5 Time-frequency filtering

Knocking creates high frequency oscillation which its amplitude decays with time. The spark knock frequency is dependent on the engine geometry and other factors. These are given by Draper's equation [6]:

$$f_r = \frac{\rho_{m,n} \cdot c}{\pi B} \tag{3.4}$$

where f_r is a resonant vibration frequency, $\rho_{m,n}$ is a vibration mode constant, c is the speed of sound (which depends on the in-cylinder instantaneous temperature), B is the cylinder radius. The different modes are different stationary wave systems [13]. The sound velocity can be calculated with Equation (3.5).

$$c = \sqrt{KRT} \tag{3.5}$$

where K is the isentropic exponent and equals 1.4, R the gas constant and equals 287 and T the average gas temperature in the cylinder [9].

For example, YANMAR TH-5 engine has a bore diameter of 80 mm. From Draper's equation (3.4), c is assumed as a constant velocity of 950 m/s, thus there are two dominant resonant frequencies at 7.0 kHz and 11.5 kHz. Figure 3.6 shows three levels of wavelet decompositions but the third level detail coefficient will only be considered, with the sampling frequency is set at 100 kHz.

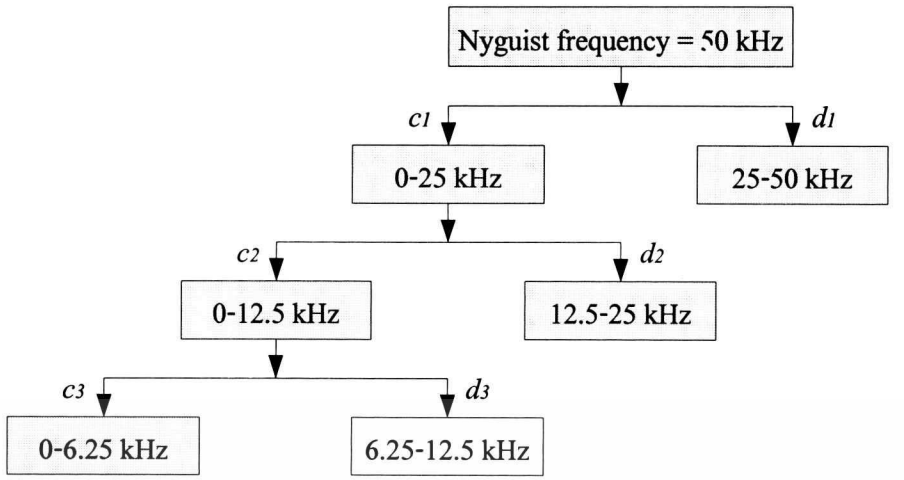

Figure 3.6 Frequency bandwidth of three levels wavelet decompositions

3.2.3 Chi-Square Statistical Threshold

Chi-square distribution is used in many statistical calculations. This statistical tool can be used to determine the precision interval of the true variance, to quantify how well a sample matches an assumed parent distribution [7]. In Equation (3.6), the statistical variable χ^2 is dependent on the number of measurements, N, at which the comparison is made. Hence, the number of degrees of freedom is $v = N - 1$. From this definition it follows that χ^2 is related to the standardized variable, z_i, and the number of measurement, N by the equation below:

$$\chi^2 = \sum_{i=1}^{N} z_i^2 \tag{3.6}$$

where

$$z_i = \frac{x_i - \bar{x}}{\sigma} \tag{3.7}$$

The idea of the thresholding procedure is to retain in the wavelet transform only the highest coefficients, which are supposed to be due to the transient signals. And putting to zero all the coefficients giving a measure of the background noise, which are smaller than a given threshold.

In this approach, Chi-square is employed to determine the set of coefficients that differs from the Gaussian distribution. The transient-related coefficients also oscillate during the time period when the transient exist. The summation of square of the transient-related coefficients is generally not distributed according to χ^2 distribution because the absolute values of the transients are much larger than those of the Gaussian components. Therefore, the transients can be detected and identified by measuring the gaussianity of the coefficient [18]. The proposed statistical process of transient threshold is shown in Figure 3.7.

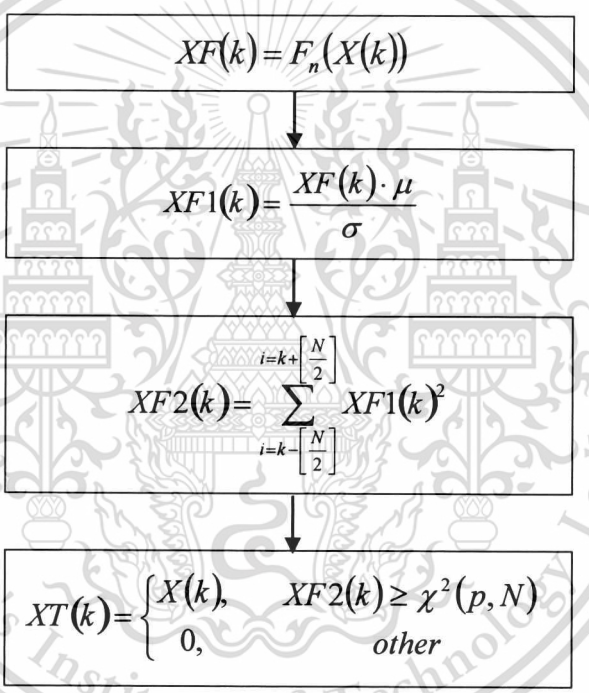

Figure 3.7 Procedure of the Chi-square statistical threshold

The details of the procedure in Figure 3.7 can be described below:

1. Calculate the statistical parameter $XF(k)$ defines as:

$$XF(k) = F_n(X(k)) \tag{3.8}$$

where $X(k)$ is the wavelet coefficients that there are n samples. If X_1, X_2, ..., X_n represent the sequential statistical series, the empirical function $F_n(x)$ is defined as:

$$F_n(x)=\begin{cases}0, & x<X_1\\ \dfrac{k}{n}, & X_k\le x\le X_{k+1}\\ 1, & x\ge X_{k+1}\end{cases} \tag{3.9}$$

2. Calculate mean μ and standard deviation σ of $XF(k)$. Then, a new time series with zero mean and unit variance is formulated through a linear transform as:

$$XF1(k)=\frac{XF(k)\cdot\mu}{\sigma} \tag{3.10}$$

3. The feature series $XF2(k)$ are the sum of square of the adjacent N points calculated as:

$$XF2(k)=\sum_{i=k-\left[\frac{N}{2}\right]}^{i=k+\left[\frac{N}{2}\right]}XF1(k)^2 \tag{3.11}$$

which satisfies χ_v^2 distribution with degree of freedom $v=N-1$ if $XF2(k)$ has standard normal distribution.

4. The transient in $XF1(k)$ can be detect based on the inverse of the χ^2 cumulative distribution function $\chi^2(p,N)$ as:

$$XT(k)=\begin{cases}X(k), & XF2(k)\ge\chi^2(p,N)\\ 0, & other\end{cases} \tag{3.12}$$

where p is a probability value that implies to significant level α, whereas $p = 1 - \alpha$.

3.3 Knock Control Strategy

This knock control strategy bases on the ignition retard control of SI engine. When knock onset in SI engine, the ignition will be retarded until no knock occur. After that, if knock disappear for a period of time, a small step of ignition advance will be applied. However, to eliminate knock in DDF engine, the reduction of alternative fuel take the place of the ignition retard. A list of steps below describes the process of knock control strategy shown in Figure 3.8.

1. If the control module hears a knock it is remembered.

2. The next time gas injection is reduced slightly.

3. If the knock continues despite, reduction the injection is reduced further the next time gas injects.

4. If there is no knock after reduction, the control module waits a short time and then increases the injection gradually.

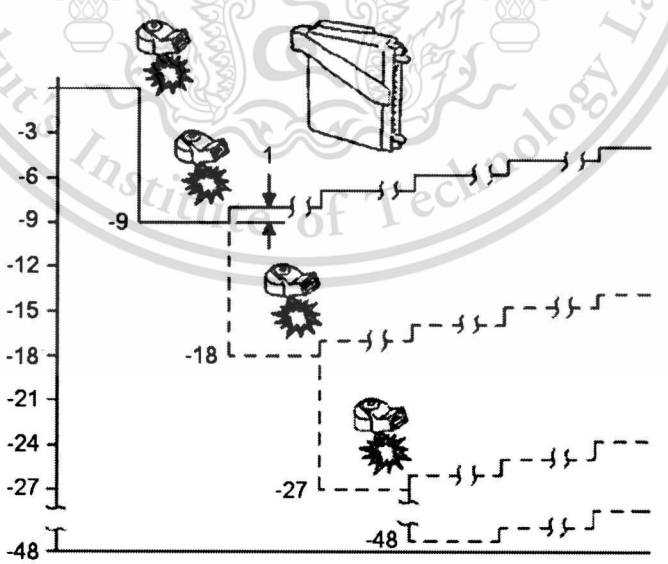

Figure 3.8 knock control strategy of DDF engine

CHAPTER 4

EXPERIMENTAL METHOD

4.1 Simulation Studies of Knock Detection

The objective of this study is to explore the distinguished performance of knock detection in noisy environment. The evaluation is to distinguish knock from each set of simulated signals with varied range of noises. In this study, there are 3 techniques to be compared, (i) band-pass filter, (ii) wavelet-based knock detection and (iii) wavelet-based knock detection with Chi-square. Each comparative method is explored to find the least value of relative error in estimating knock intensity $\delta_{\%}$. Regarding to the comparison of the different knock feature extraction domains, the knock features in wavelet coefficients domain must be inversed transform to the time series signal, referring to each other. Hence, in this case study, the knock intensity, KI is defined by Equation (4.1).

$$KI = \sum_{t} |y(t)| \tag{4.1}$$

where, $y(t)$ is the knock evaluation signal of the simulated signal, and t is the time in series of the signal.

The relative error in estimating knock intensity $\delta_{\%}$ defines as Equation (4.2).

$$\delta_{\%} = \frac{KI_{SNR} - KI_{Clean}}{KI_{SNR}} \times 100 \tag{4.2}$$

where, KI_{SNR} is knock intensity of the simulated signal with an addition of noise at a specific SNR, and KI_{Clean} is knock intensity of the simulated signal without any addition of noise.

As shown in Equation (4.2), the relative error in this case is not an absolute value. The minus value of $\delta_{\%}$ means that KI_{SNR} (from the signal with additional noise) is less than KI_{Clean} (from the signal without noise). This implies that the knock evaluation signal is attenuated during process.

4.1.1 Simulation Signals

To evaluate the knock detection methods, an analytically formulated signal is used. The signal $s(t)$ consists of decaying oscillating component $s_1(t)$, periodic component $s_2(t)$, and Gaussian-modulated sinusoidal pulse $s_3(t)$. It is also interfered by white Gaussian noise $s_n(t)$, [18].

$$s(t) = s_1(t) + s_2(t) + s_3(t) + s_n(t), \quad t \in [0 - 0.7] \tag{4.3}$$

where

$$s_1(t) = \begin{cases} 3e^{-30|t-0.15|} \sin 2\pi f_k (t - 0.1), & t \in [0.1 - 0.2] \\ 0, & other \end{cases} \tag{4.4}$$

$$s_2(t) = \begin{cases} 2\sin 2\pi f_k (t - 0.3), & t \in [0.3 - 0.4] \\ 0, & other \end{cases} \tag{4.5}$$

$$s_3(t) = \begin{cases} 2e^{\frac{-(t-0.55)^2}{0.0009}} \cos 2\pi f_k (t - 0.55), & t \in [0.5 - 0.6] \\ 0, & other \end{cases} \tag{4.6}$$

and

$$s_n(t) \sim N(0,1), \quad t \in [0-0.7] \tag{4.7}$$

To obtain more precise results, the signal $s(t)$ is repeatedly generated with sampling frequency of 40 kHz for several SNRs varying from 1 to 40 dB with the increment of 1, and the supposed transient frequency f_k = 15 kHz is used as the knock frequency. Some simulated signals, with SNRs of 20 dB, 10 dB and 0 dB, are showed in Figure 4.1.

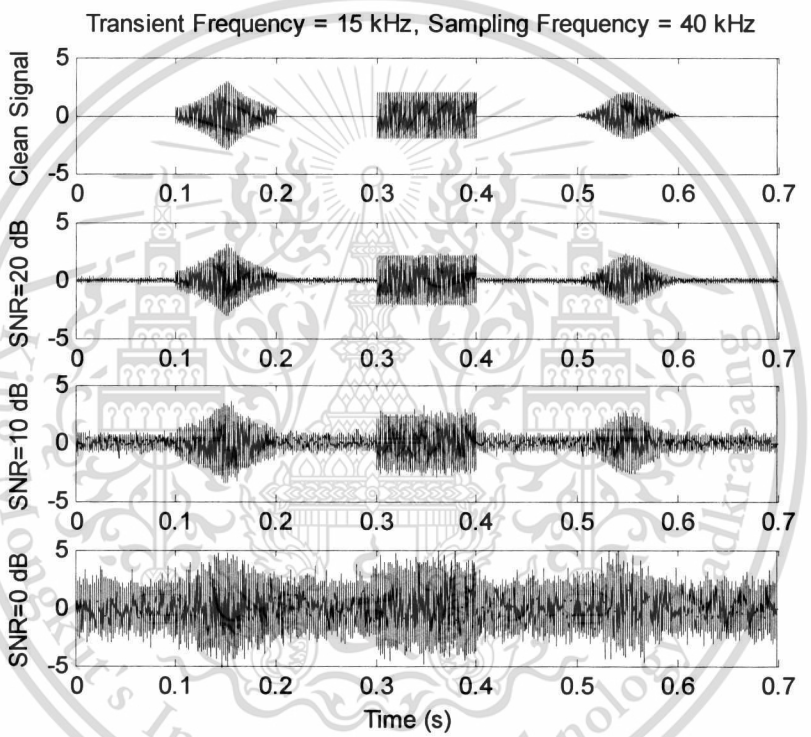

Figure 4.1 Simulated signals with various noise levels.

4.1.2 Band-Pass Filter Method

The filters used were created using MATLAB's Filter Design and Analysis Tool (FDATool). This toolbox is a user interface that easily allows the user to input all of the necessary filter parameters including filter type, design method, order, frequency specifications and magnitude specifications. The tool then designs the filter and the filter coefficients can be exported to a text file to be used in combination with a

filter command in a MATLAB program. The orders and the frequencies of all filters used in this study can be found in Table 4.1.

Table 4.1 Band-pass filter specifications

Filter No.	first stop [kHz]	first pass [kHz]	second pass [kHz]	second stop [kHz]	order
1	13.5	14.5	15.5	16.5	50
2	13.5	14.5	15.5	16.5	100
3	13.5	14.5	15.5	16.5	200
4	14.25	14.75	15.25	15.75	200
5	14.8	14.9	15.1	15.2	200

All filters used in Figure 4.2 are finite impulse response (FIR) equiripple band-pass filter with the density factor of 16 and the sampling frequency of 100 kHz. The magnitude specifications are 60 dB for the first stop, 1dB for the pass, and 80 dB for the second stop.

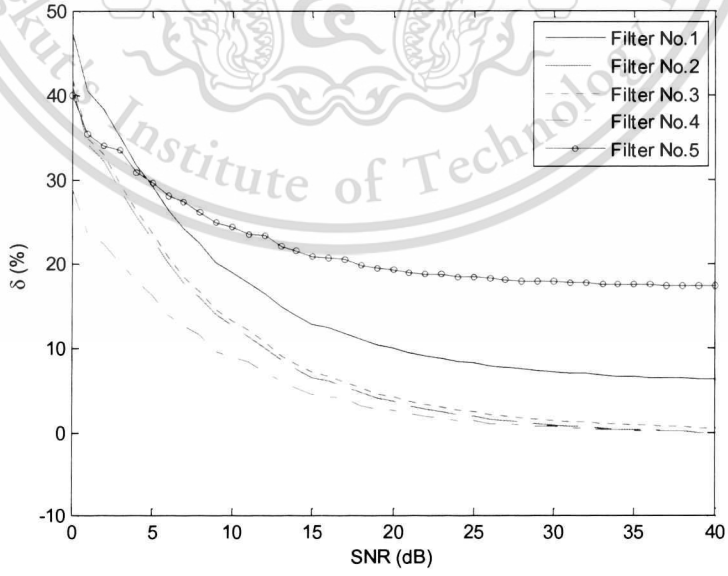

Figure 4.2 Relative error in estimating knock intensity versus SNR of band-pass filter method.

The simulation results show that the traditional knock detection using band-pass filter is effective only at low noise level, as shown in Figure 4.2. For the best in class, filter No. 4 shows the least error in knock estimation. At 40 dB, it gives the smallest error and the error is growing if the noise level is higher.

4.1.3 Wavelet-Based Knock Detection Method

The knock detection performance of non-statistical wavelet-based is showed in Figure 4.3. The results demonstrate that with the threshold level P = 2.0, the wavelet-based technique can improve the performance of knock detection at high noise level, which the band-pass filter cannot do. For instance, at SNR = 0 dB with P = 2.0, the error is just around 3%. However, when the SNR increases, the error is increased from 3% to about -40%. Thus, the threshold level P should be set according to the SNR level.

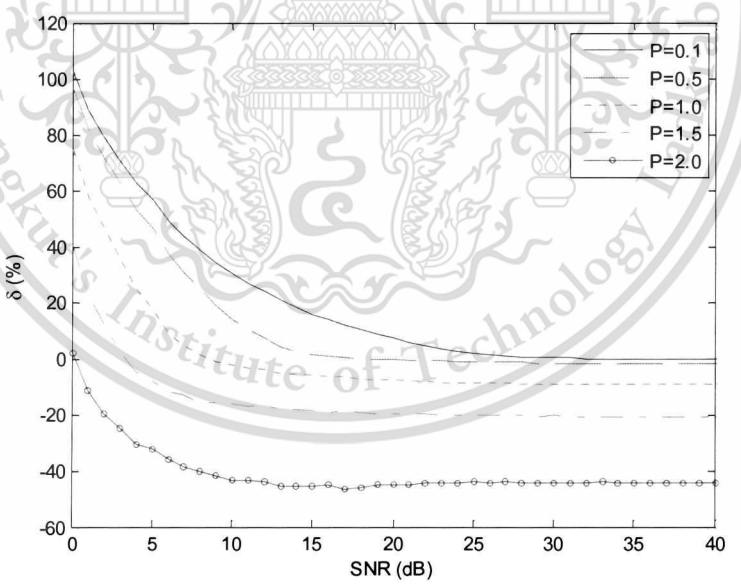

Figure 4.3 Relative error in estimating knock intensity $\delta_{\%}$ versus SNR of non-statistical wavelet- based knock detection method.

4.1.4 Wavelet-Based Knock Detection with Chi-Square Method

The results, in Figure 4.4, show that the proposed method can sense knock feature very effectively in wide SNR range. With a significant level α = 0.3, the error is less than 4% for 0 to 40 dB SNR levels.

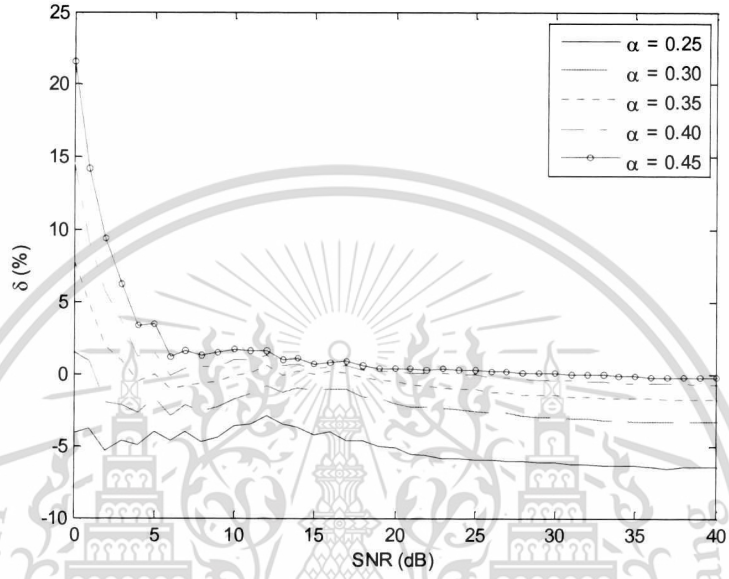

Figure 4.4 Relative error in estimating knock intensity $\delta_{\%}$ versus SNR of wavelet-based knock detection with Chi-square method.

4.1.5 Comparison of the Studied Knock Detection Method

The best results of each technique were selected and plotted in Figure 4.5 for comparing. It is obviously clear that the proposed wavelet-based knock detection with statistical Chi-square method performed well in all SNR ranges. For the native wavelet-based method, it gives a good result in some specific SNR, even at very high noise level (i.e. P = 2.0), whereas the band-pass filter method is effective only at high SNR.

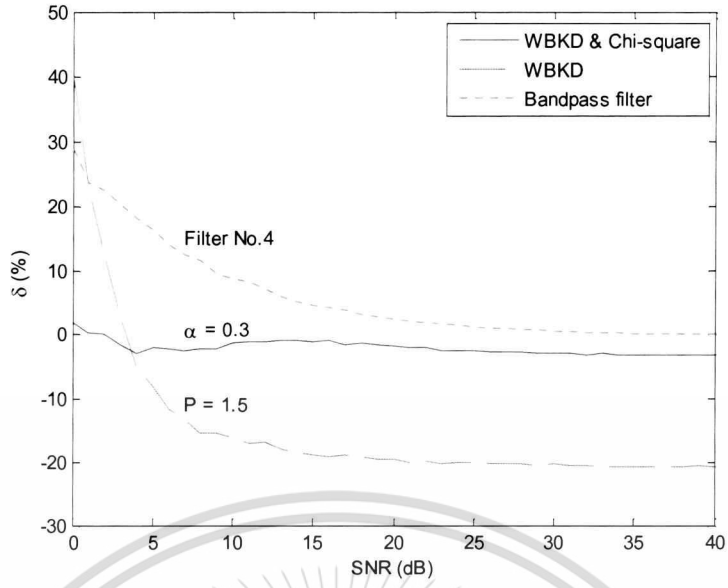

Figure 4.5 Comparison of 3 knock detection techniques.

4.2 Experiment of Knock Detection

In this experiment, the wavelet-based knock detection with Chi-square, which is the best among all techniques, was selected to evaluate performance on the real DDF system. Figure 4.6 shows the engine used in this experiment.

Figure 4.6 YANMAR TH-5 experimental engine

4.2.1 Engine Specification

The knock detection was applied on YANMAR TH-5, a small single cylinder, indirect injection (IDI) diesel engine. The engine specification is showed in Table 4.2.

Table 4.2 YANMAR TH-5 engine specification

Type	4 strokes diesel
Displacement	223 cc
Bore	80.0 mm
Stoke	44.5 mm

4.2.2 Diesel Dual Fuel Setup

For the tests, the engine was modified to operate as the DDF engine by allowing gas and air mixed in the air intake duct with no adjustment for amount of diesel injection. The additional non-resonant knock sensor was mounted on the engine housing to sense the vibration signal.

4.2.3 Knock Measurement

In each test, the engine is fully warmed-up to meet the operating temperature. The DDF knock condition was performed by keeping constant amount of diesel fuel while increasing the amount of LPG until the spark knock onset. Data were acquired for off-line processing by using NI PCI-6024E data acquisition system, at a sampling rate of 100 kHz. In this test, 69 combustion cycles were recorded at an engine speed of 520 RPM, regarding to where the knock begins.

4.2.4 Data Processing and Analysis

The proposed method was applied to detect the knock from entire combustion cycles. The significant level α = 0.05 was chosen for gaussianity test. Knock intensity was calculated based on the transient feature evaluation in wavelet coefficient domain. The combustion was determined as knocking if the knock

intensity greater than a threshold --- a half of mean value of the last five values that were a knock combustion.

4.2.5 Knock Detection Results

The experimental results show that there are 7 knock cycles, #8, #11, #19, #22, #35, #56, and #64, detected by the wavelet-based with Chi-square method shown in Figure 4.7. The waveform of the knock combustion cycles illustrated in Figure 4.8 (a) shows the original vibration signals which correlates to its transient coefficients of knock combustion shown in Figure 4.8 (b). In these figures, they consist of 4 peaks in each plot that involve in EVC, IVC, knocking and ignition periods, from left to right respectively.

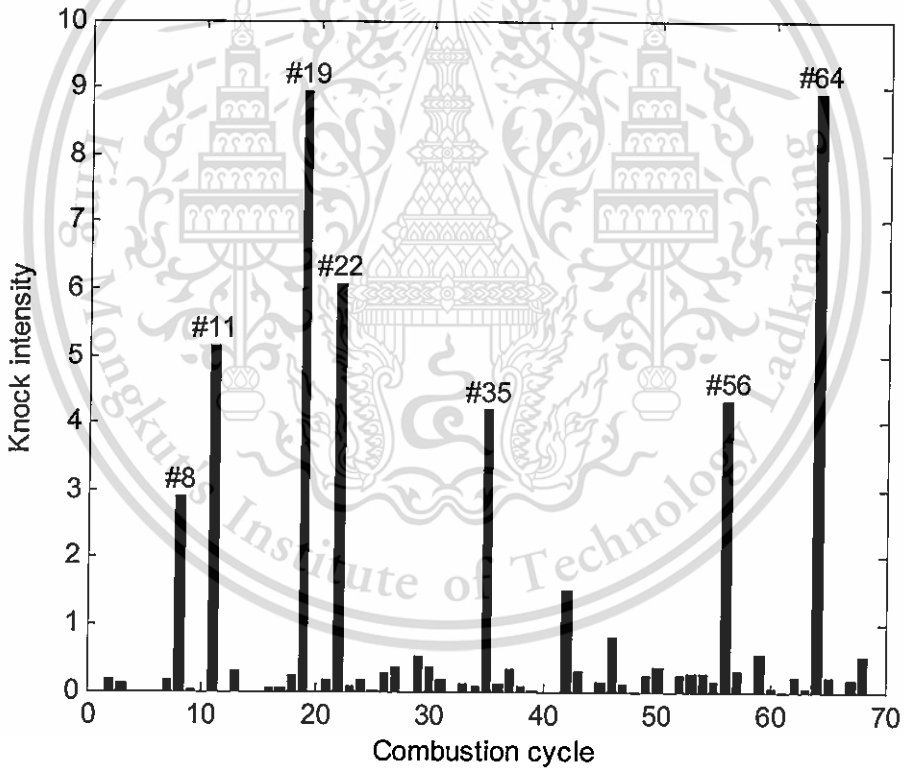

Figure 4.7 Knock intensity detected from 69 combustion cycles.

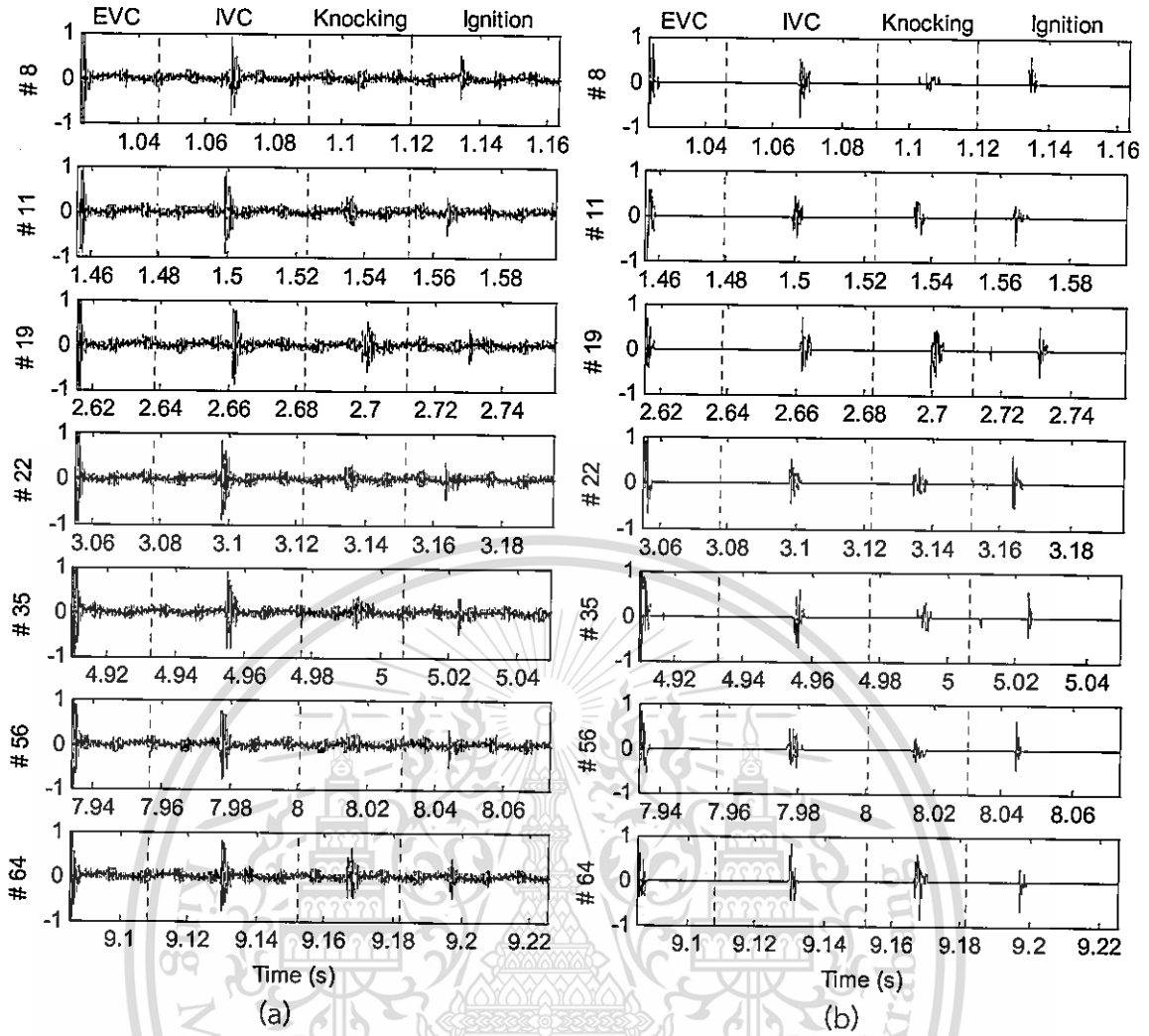

Figure 4.8 Waveform of knock signals on a YANMAR TH-5: (a) time domain vibration signal, (b) transient filtered by using wavelet-based knock detection with Chi-square.

4.3 Experiment of Knock Control

The DDF system mostly uses CNG, of which the price is lower than others, as the alternative fuel. Since the spark knock of using CNG usually occurs when the temperature of the combustion chamber is too high, this circumstance is not suitable for using as a control stage; thus, this knock control experiment deals with the control of the diesel knock, which always occurs before the spark knock, in the DDF operations.

4.3.1 Engine Specification

The engine used in this experiment is on a test car (1998 Ford Ranger). This engine has known as Ford 2500 WL-T turbocharged diesel engine. The engine specification can be found in Table 4.3.

Table 4.3 Ford 2500 WL-T engine specification

Type	4 strokes diesel with turbocharger
Displacement	2499 cc
Bore	93.0 mm
Stoke	92.0 mm
Compression Ratio	19.8:1

4.3.2 Diesel Dual Fuel Setup

The experimental diesel engine has been modified to operate as DDF engine by the additional DDF conversion kits. The important part is the gas injectors and the electronic control unit (ECU). There are two gas injectors that were mounted to inject CNG into the inlet manifold, Figure 4.9 (b). CNG was injected twice per engine cycle by alternating each injector by one at a time. Timing and duration of CNG injection, which vary due to different engine speeds and loads, are controlled by the ECU from NECTEC. The gas injection pulse width, which refers to the amount of CNG supplement, can be adjusted by DDF calibration software as the engine was running. The additional non-resonant knock sensor was mounted on the engine housing to sense the vibration signal. The location of the knock sensor is showed in Figure 4.9 (a).

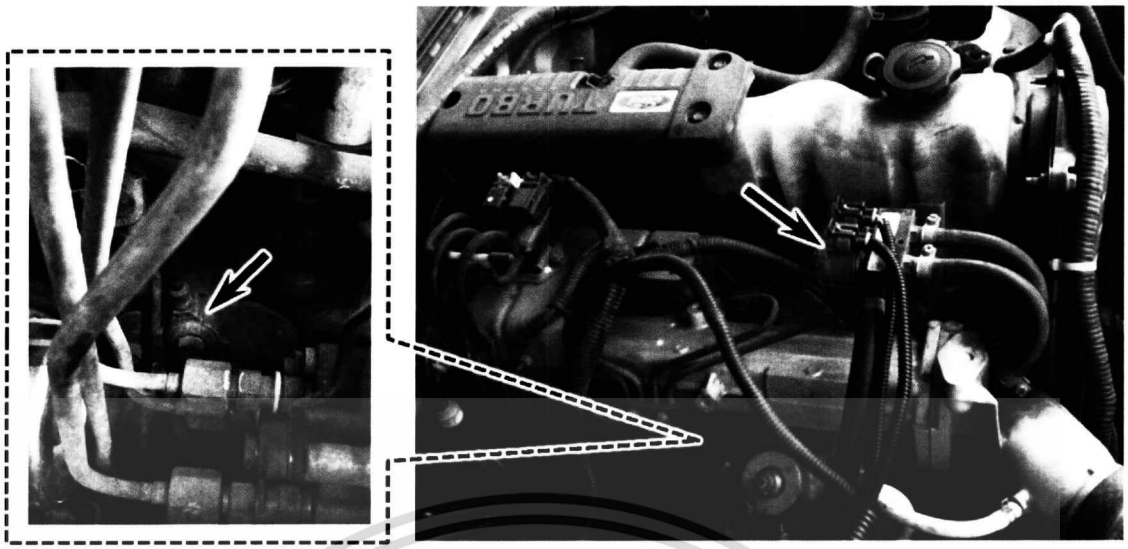

(a) (b)

Figure 4.9 Additional components on Ford Ranger engine: (a) knock sensor (arrowed), (b) two gas injectors (arrowed).

4.3.3 NECTEC-DDF Calibration Software Modification

The users are allowed to configure NECTEC-DDF ECU via NECTEC-DDF calibration software. In the traditional DDF system as well as in the original version software, only the gas injection table shown in Figure 4.10 appears for adjusting. The values contained in this table relate to the gas injection pulse width.

Since the new approach knock control algorithm was applied, the knock calibration table has been added to the original software for compensation with the gas injection table, Figure 4.11. The correlative values between both tables are referenced by the coordination of speed (x-axis) and load (y-axis) of the engine operations.

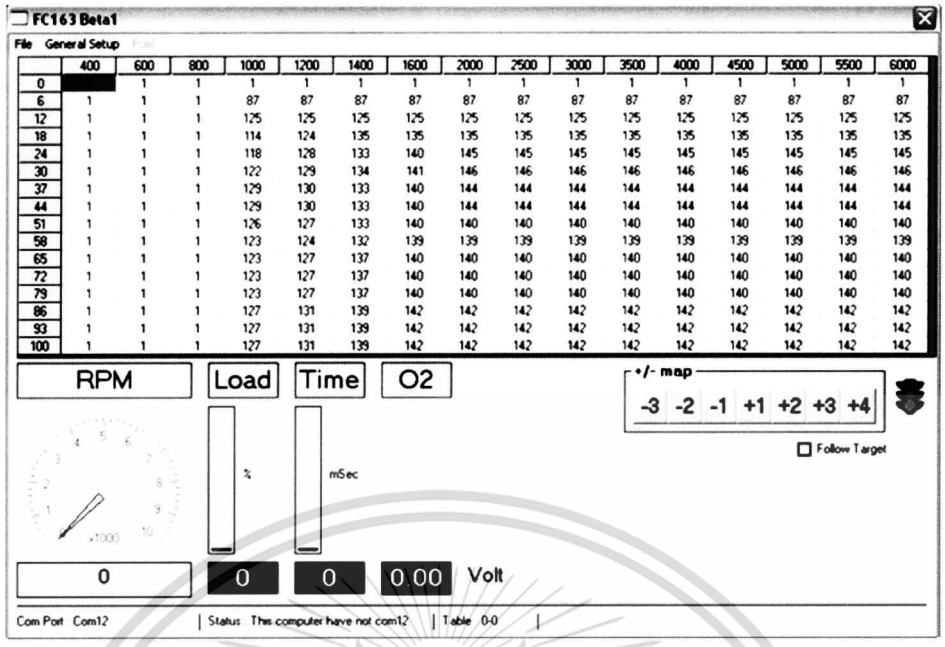

Figure 4.10 Original version of NECTEC-DDF calibration software

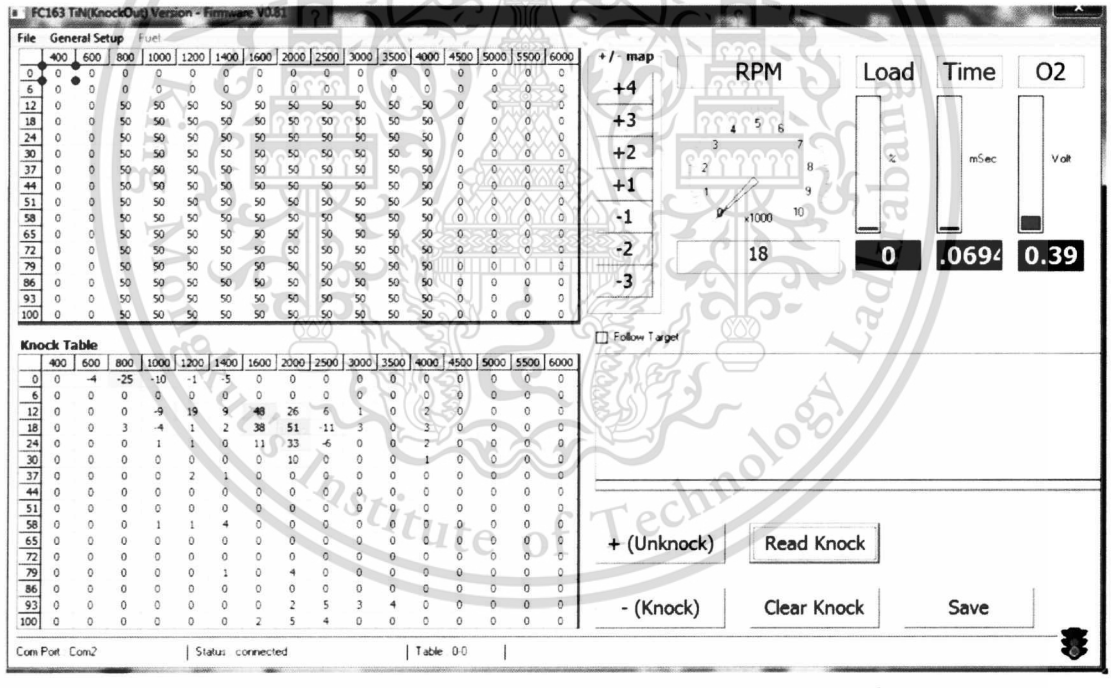

Figure 4.11 Modified version of the DDF calibration software

4.3.4 NECTEC-DDF ECU Firmware Modification

The original firmware of NECTEC-DDF ECU shown in Figure 4.12 is not compatible for the knock compensation, so the new firmware including the array of knock calibration values has been updated to support the new properties.

Furthermore, some protocols also have been added in order to communicate with both of the modified version of calibration software and the additional knock control module. The microcontroller used in NECTEC-DDF ECU is dsPIC30F6014 from Microchip, and the firmware was written in C.

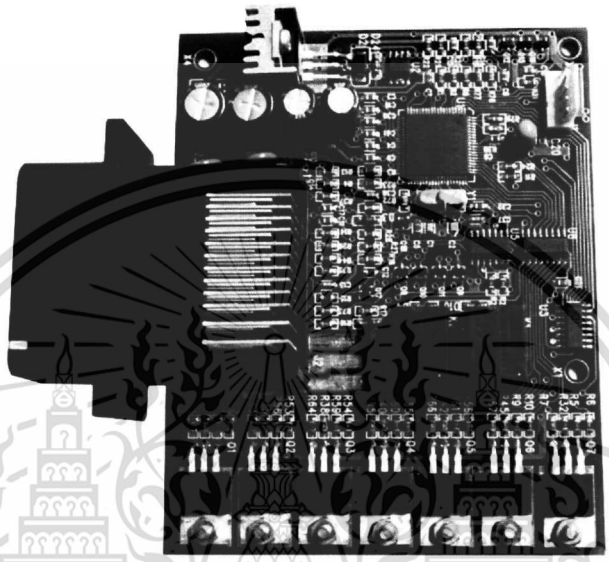

Figure 4.12 NECTEC-DDF ECU

4.3.5 Knock Control Module Setup

The knock control module consists of the data acquisition module and the knock control application running on notebook. The data acquisition module NI USB-6225 was used to acquire data. It provides one digital input channel and two analog input channels. The digital input is the CNG injection signal, which is the one of the outputs from DDF ECU. The analog inputs are those of the vibration signal from a knock sensor and the throttle position signal from a throttle position sensor (TPS). All data were acquired at a high acquisition speed of 100 kHz. The acquired data were processed by the knock control application, and the outputs are sent to DDF ECU as the updated knock values for compensation to the gas injection pulse width.

4.3.6 Power and Torque Operating Conditions

In DDF system, the amount of alternative fuel injection is varied due to the engine operation according to the engine speed and load. Regarding to the fact that the engine does not require any additional power for the operations of idle speed and during deceleration, mean that the alternative fuel will be needed to supplement together with diesel fuel only during the power and torque operating conditions. The graph shown in Figure 4.13 illustrates the power and the torque outputs of the test engine.

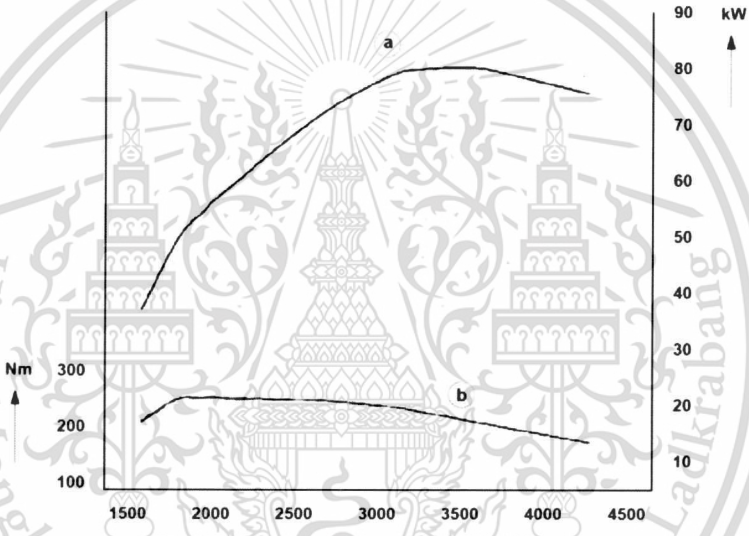

Figure 4.13 Power and torque graph of Ford 2500 WL-T: (a) power output, (b) torque output

4.3.7 Experimental Procedure

Before beginning any experiment, the test car was warmed up to reach the normal operating temperature. A list of the steps below was taken in order to get the updates of knock calibration table.

1. Adjust the gas injection pulse width via NECTEC-DDF calibration software by using the initial values for the gas injection table and clear any values of the knock table to zero. The initial values were assigned as shown in Table 4.4.

2. Make an initial of control parameters, such as the knock threshold and the decreasing step of the knock calibration value, for the knock control application from previous trends.

3. Setup the knock control module and then connect to NECTEC-DDF ECU. After that, run the knock control application.

4. On the road test with the normal driving condition and considering about the conditions of idle speed, on/off the air conditioner and up/down the hill. Care should be taken to avoid a rising of engine temperature or any extreme knocking condition that might lead to the engine damage.

5. After driving, reconnect to NECTEC-DDF calibration software again to check the knock table which had been updated.

Table 4.4 Initial values of gas injection table

	400	600	800	1000	1200	1400	1600	2000	2500	3000	3500	4000	4500	5000	5500	6000
0	0	0	0	0	0	0	0	0	0	0	0	0	0	0	0	0
6	0	0	0	0	0	0	0	0	0	0	0	0	0	0	0	0
12	0	0	50	50	50	50	50	50	50	50	50	50	0	0	0	0
18	0	0	50	50	50	50	50	50	50	50	50	50	0	0	0	0
24	0	0	50	50	50	50	50	50	50	50	50	50	0	0	0	0
30	0	0	50	50	50	50	50	50	50	50	50	50	0	0	0	0
37	0	0	50	50	50	50	50	50	50	50	50	50	0	0	0	0
44	0	0	50	50	50	50	50	50	50	50	50	50	0	0	0	0
51	0	0	50	50	50	50	50	50	50	50	50	50	0	0	0	0
58	0	0	50	50	50	50	50	50	50	50	50	50	0	0	0	0
65	0	0	50	50	50	50	50	50	50	50	50	50	0	0	0	0
72	0	0	50	50	50	50	50	50	50	50	50	50	0	0	0	0
79	0	0	50	50	50	50	50	50	50	50	50	50	0	0	0	0
86	0	0	50	50	50	50	50	50	50	50	50	50	0	0	0	0
93	0	0	50	50	50	50	50	50	50	50	50	50	0	0	0	0
100	0	0	50	50	50	50	50	50	50	50	50	50	0	0	0	0

4.3.8 Data Processing and Analysis

The experimental data, which were recorded in the category of speed and load coordination, were used to analyze the knock control results and calculate other relevant parameters. This section contains a summary of the successful data processing and analysis methods found throughout the proposed knock control strategy.

4.3.8.1 Determining the Knock Window

For the accuracy and reduction of computation, the knock window is used as a time selection for considering only the interested sections of the signal. In general, the knock window usually associates with the degree of crank angle (CA). For instance, in SI engine, typically the knock occurs near top dead center (TDC) and ends about 70° after top dead center (ATDC) [8]. Therefore, an execution window should be comprising 60° of the crankshaft angle as located at 10° - 70° CA ATDC for the monitoring period.

The recorded signal shown in Figure 4.14 is the vibration signal from the test car during a driving test. The signals with high amplitude, which are used to classify between knock and normal combustion, are the vibrations while the combustion occurs. When considering only the combustion signal, the background noise appears to be low overall engine cycle. Moreover, it becomes such a good signal quality when compared with the previous experiment taken on a small single-cylinder diesel engine. The obvious background noises such as EVC and IVC were disappeared because of a longer distance between the noisy source (engine valve) and the knock sensor location.

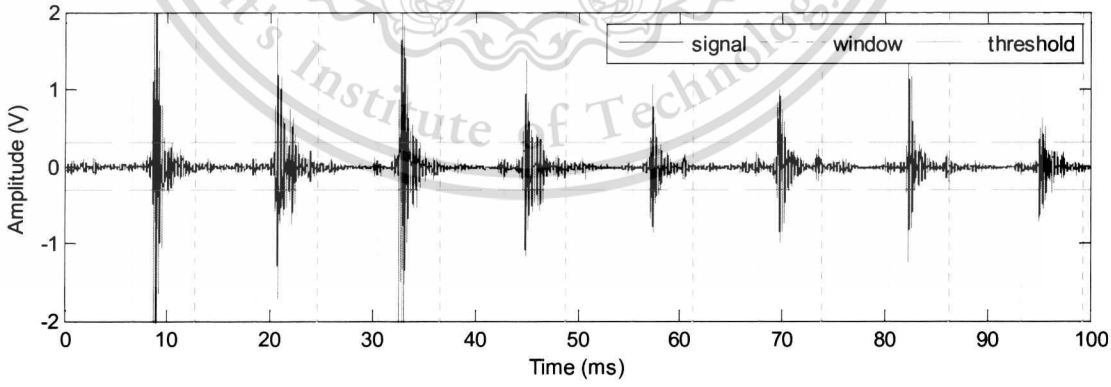

Figure 4.14 Window positions of the vibration signal with level threshold

Figure 4.14 illustrates the green horizontal lines as a threshold level, whereas the red vertical lines are the knock window of each monitoring signal. The waveforms shown in Figure 4.15 are the signal inside the knock windows from Figure 4.14 in

order from left to right. Since the test engine does not have a cam position sensor, the knock window cannot associate with the degree of crank angle. However, in case of the high differential amplitude between the combustion signal and the others as shown in Figure 4.14, the level thresholding is effective enough to locate the knock window.

See Figure 4.15, each plot has the same range of x-axis and refers to the window length of 6 milliseconds. The suitable length of the monitoring window can affect the accuracy of knock evaluation. Thus, in this experiment, the optimal window length should be selected for 4 milliseconds.

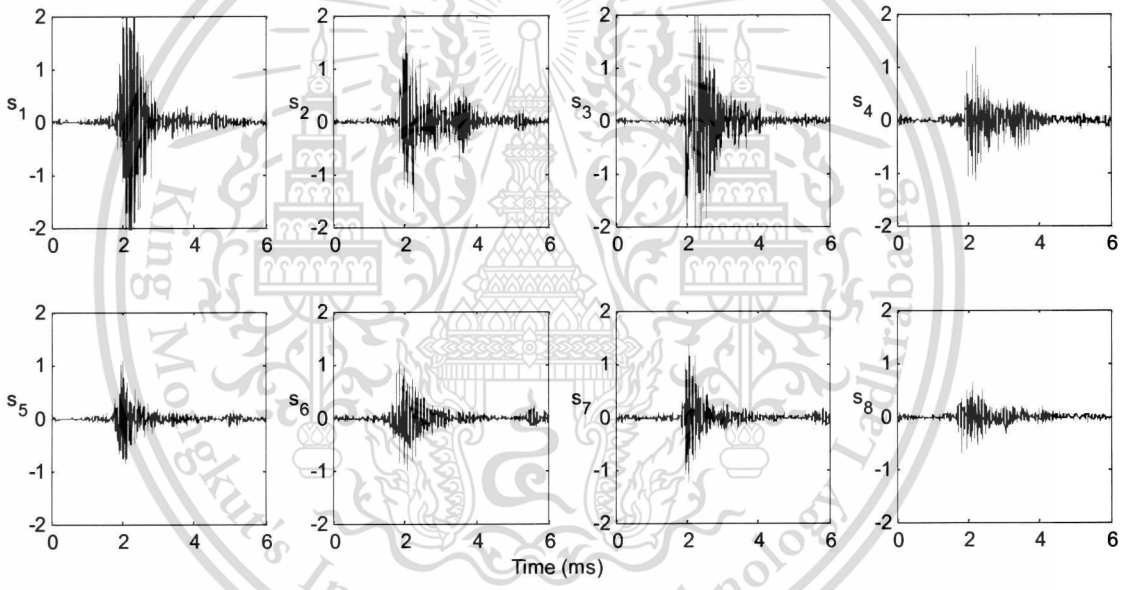

Figure 4.15 Windowed signal from Figure 4.14, order by left to right

4.3.8.2 Signal Decomposition Using Wavelet Lifting Scheme

As mentioned in the beginning of CHAPTER 3 that knock will be resulted in multi-stages of the ignition and the combustion processes of the vibration signal. Accordingly, Figure 4.16 (b) shows the vibration signal with knock, and can be compared with Figure 4.16 (a) showing the vibration signal without knock. In the case of knock, the combustion seems to be bad noticed from the amplitude reduction of

the vibration signal as the result of the replacement of O_2 by large quantities of CNG.

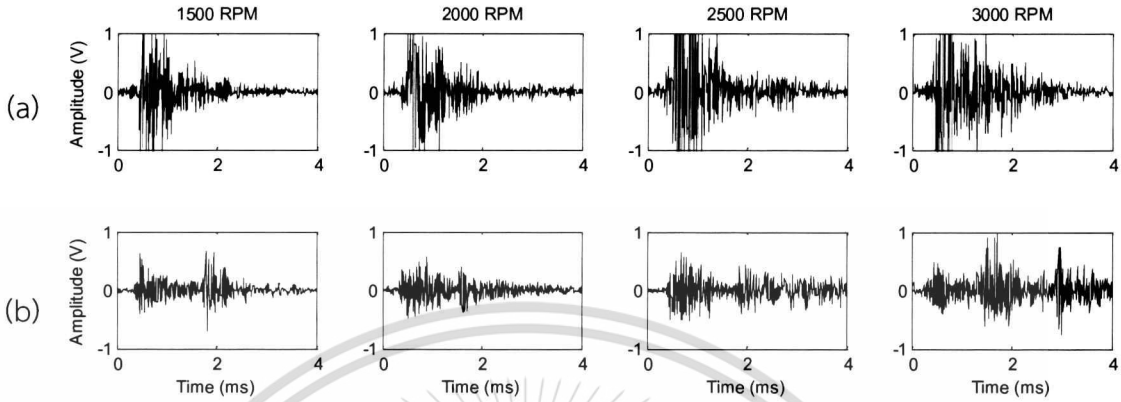

Figure 4.16 Waveform of the vibration signal at the speeds of 1500, 2000, 2500 and 3000 RPM: (a) signal without knock, (b) signal with knock

To obtain the difference in term of frequency between the vibration signals from no knock (normal) and knock combustion, so FT is employed to represent both comparative signals in frequency domain. Figure 4.17 (a) and Figure 4.17 (b) show the power spectrums of comparative signals in Figure 4.16 (a) and Figure 4.16 (b), respectively. The results show that the high amplitude of the power spectrums appear further from 20 kHz in Figure 4.17 (a) but absent in Figure 4.17 (b) for the varying speeds of 1500, 2000, 2500 and 3000 RPM.

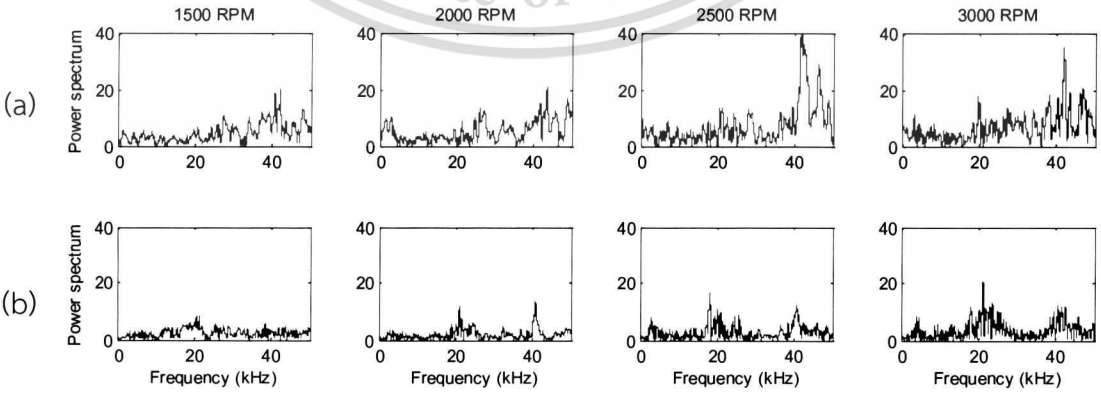

Figure 4.17 FT of the signal in Figure 4.16: (a) signal without knock, (b) signal with knock

In this experiment, the sampling frequency was set at 100 kHz, and a known frequency of interest is around 20 kHz and higher; hence, it concerns two levels of wavelet decompositions for dealing with the coefficients d_1 and d_2. The decomposition tree on two levels is given below in Figure 4.18.

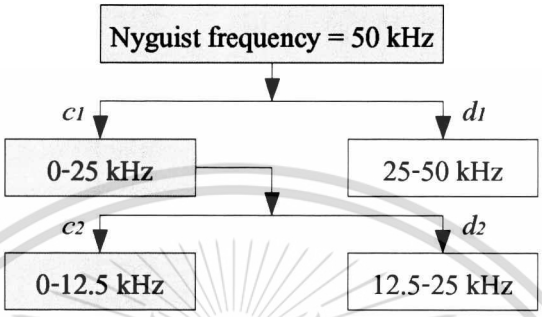

Figure 4.18 Frequency bandwidth of two levels wavelet decompositions

In the proposed method, the Daubechies orthogonal wavelet with 8 vanishing moments (db8) is used to decompose the vibration signal. The waveforms of the vibration signals with varying speeds of 1500, 2000, 2500 and 3000 RPM with its wavelet expansion coefficients are represented in Figure 4.19, in case of knock, and in Figure 4.20, in case of no knock. The notations are: s - the original signal, d_1, d_2, c_2 are wavelet coefficients.

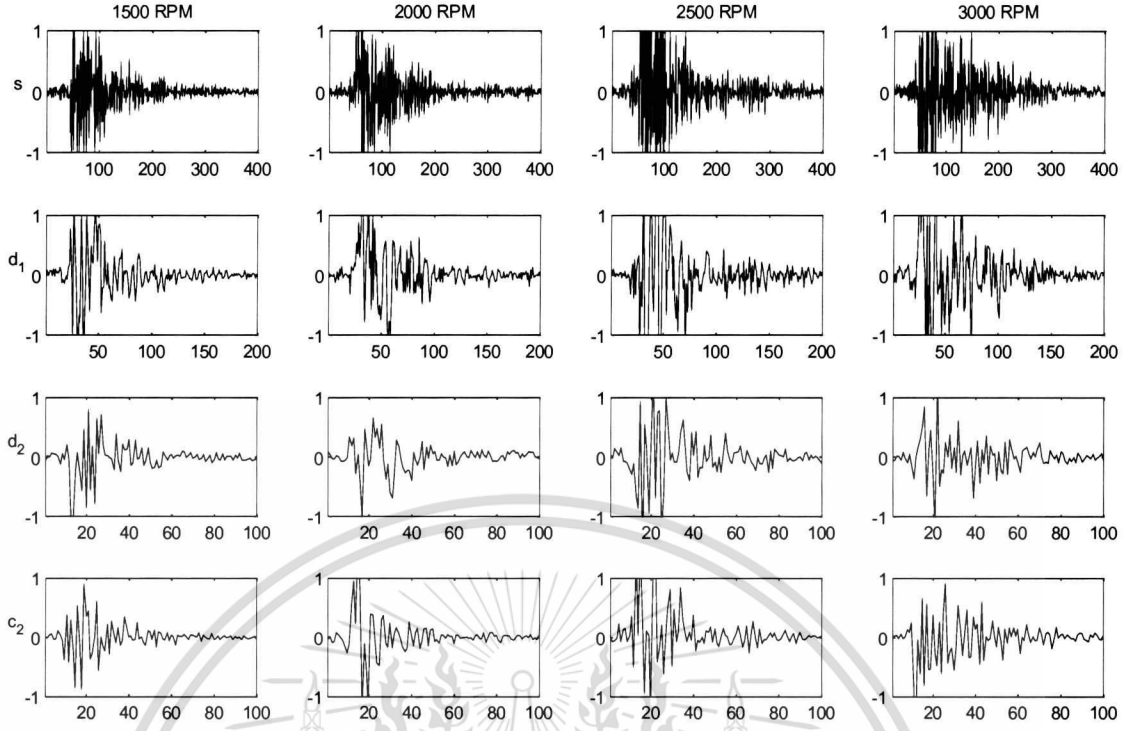

Figure 4.19 Waveforms of wavelet decomposition at level 2 of the signals without knock

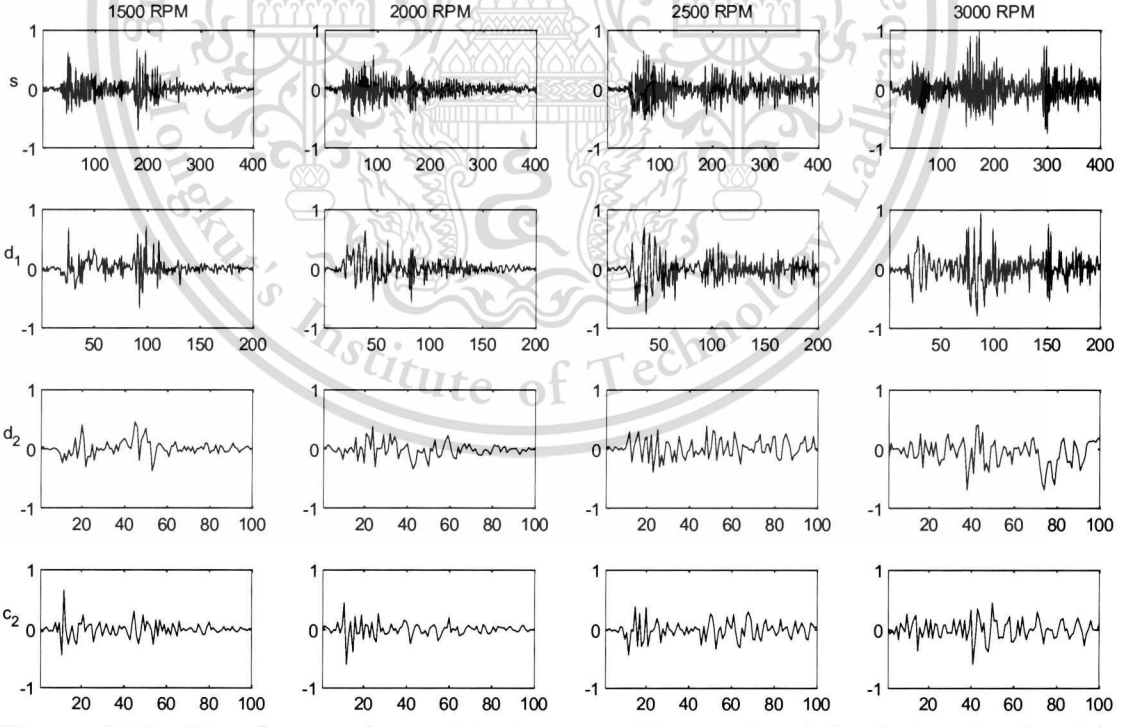

Figure 4.20 Waveforms of wavelet decomposition at level 2 of the signals with knock

4.3.8.3 Identify the Transient Feature Using Chi-Square

Regarding to the results of the simulation study and the previous experiment of knock detection, Chi-square technique is very useful to extract the transient features of the vibration signal. Although this technique can be effective against wide SNR range, the specific significant level α has to be considered to appropriate the SNR range according to the engine operation. See Figure 4.21, showing the comparison of the signals energy compute based on wavelet coefficients d_1 and its transient features XT_1 obtaining from the application of Chi-square with α = 0.1. The signals s to be considered are: the vibration of the engine speed of 2500 RPM, Figure 4.21 (a), and varying SNR of 20 dB and 15 dB, Figure 4.21 (b) and Figure 4.21 (c), respectively. The results demonstrate that when using Chi-square, the difference in energy of transient features XT_1 is very low, but without using Chi-square, the energy of d_1 varies too much according to the SNR levels. For instance, the difference in energy between original signal with SNR of 15 dB between Figure 4.21 (a) and Figure 4.21 (c) are 13.09 for d_1, but only 1.14 for XT_1.

In this experiment, as the test engine can perform the good quality of the vibration signal (e.g. SNR > 20 dB), the significant level α was assigned to 0.1 for the Chi-square transient extraction. Hence, the estimation of knock will deal with the transient features of wavelet coefficients XT for the best accuracy.

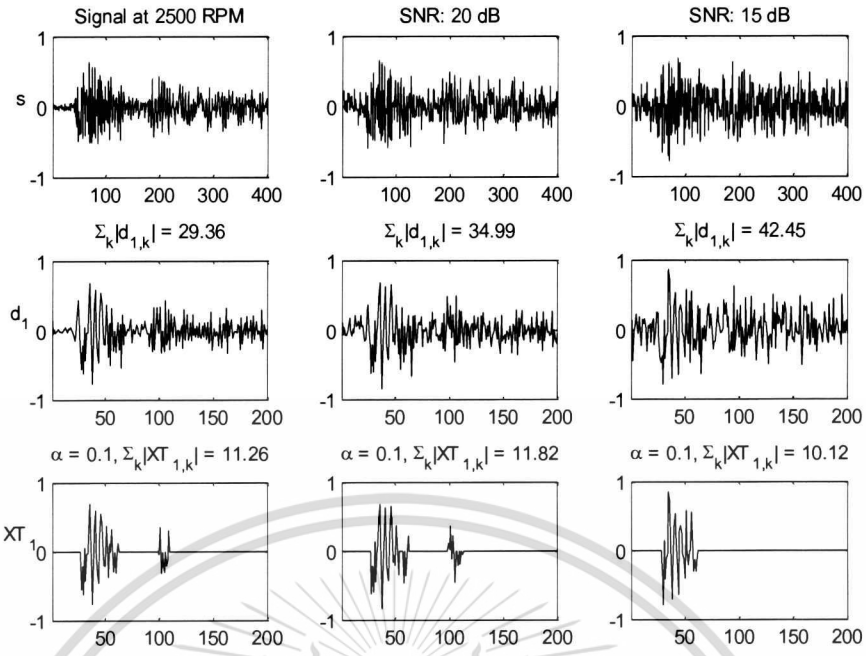

Figure 4.21 Transient feature extraction of coefficient d_1 from varying SNR signals: (a) original signal, (b) noise addition with SNR of 20 dB, (c) noise addition with SNR of 15 dB

4.3.8.4 Knock Estimation

Because of orthogonality of the decomposition, the energy of the signal can be computed based on wavelet expansion coefficients (Parseval's theorem) [8]. Thus, according to Equation (4.8), knock estimation KE is defined by:

$$KE = \sum_j \sum_k d_{j,k}^2 \tag{4.8}$$

where, $d_{j,k}$ is the detail coefficient after time-frequency filtering and thresholding, which correspond to the transient feature $XT_{j,k}$ in the proposed method.

The knock estimation (KE) is to distinguish the knock from the normal combustions. In this case, the treatment data are used as the reference to classify

between the normal and the knock regions. There are 2 sets of treatment data which are handled as follows: (i) normal condition by using pure diesel fuel operation, (ii) knock condition by using large quantity of CNG in dual fuel operation. The relevant coefficients in this experiment are d_1 and d_2. The estimated knock values, which are calculated from the transient features of relevant coefficients at the speed of 3000 RPM for 200 combustion numbers of each treatment data set, are plotted in Figure 4.22, Figure 4.23 and Figure 4.24.

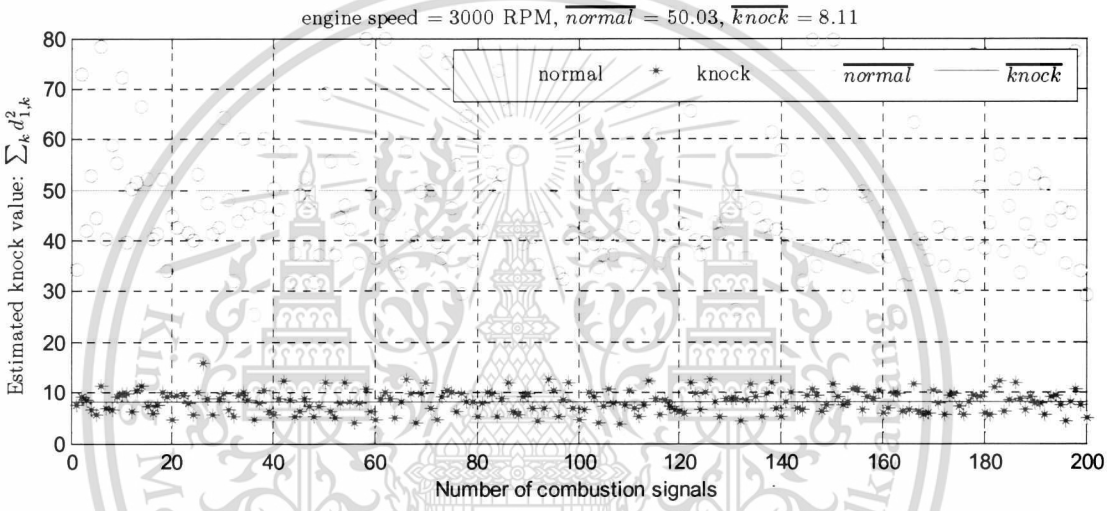

Figure 4.22 Estimated knock values of coefficients d_1 from treatments data

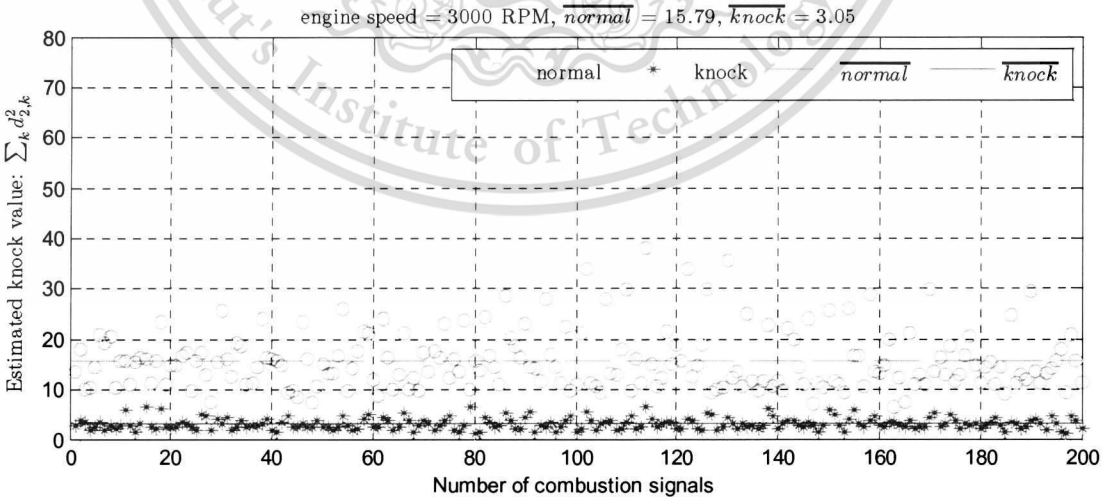

Figure 4.23 Estimated knock values of coefficients d_2 from treatments data

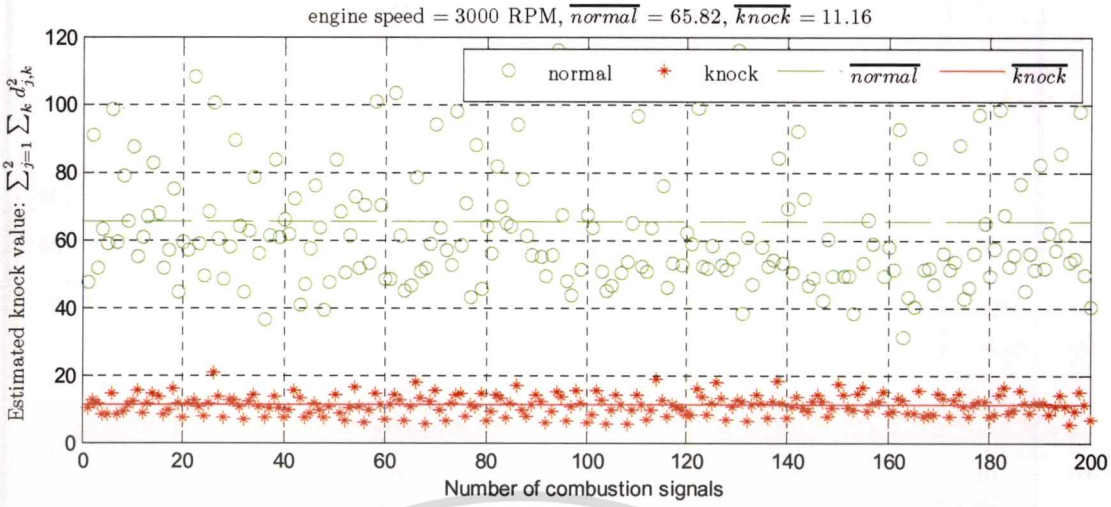

Figure 4.24 Estimated knock values of coefficients d_1 and d_2 from treatments data

As shown in Figure 4.22, Figure 4.23 and Figure 4.24, the plots of KE can be divided into two regions which are: (i) normal region, including by the O-marks, (ii) knock region, including by the asterisk marks (*). In each figure, the $\overline{normal}$ line and the $\overline{knock}$ line are the mean of KE values from 200 combustion numbers of each treatment data set according to the normal and the knock conditions. There are three computations of KE which are illustrated by those of the figures above: Figure 4.22 represents the energy of d_1, Figure 4.23 represents the energy of d_2 and Figure 4.24 represents the summation of energy of d_1 and d_2.

The plots in Figure 4.22 show that the knock zone is distinctly separated from the normal zone and can be compared with Figure 4.23 which the separation is more closely. The reason is that the difference between the normal and the knock signals contains mostly in the frequency band of d_1 but less in d_2. As shown in Figure 4.24, the knock estimation using the combination of d_1 and d_2 can extend the region of separated zone. In this case, to reduce the excessive computation, only the energy of d_1 is effective enough to classify between the knock and the normal regions. The energy representations of d_1 from the treatment data sets in the cases of engine speeds of 1500, 2500 and 3000 RPM are illustrated in Figure 4.25 (a), Figure 4.25 (b) and Figure 4.25 (c), respectively.

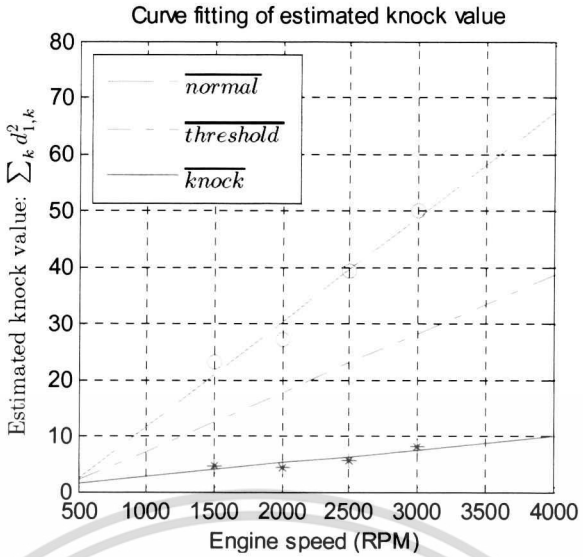

Figure 4.26 Curve fitting of the mean value of KE versus speed from the treatment data sets

4.3.8.5 Table Update Method for Knock Control

The concept of the knock table update method is to adjust the gas injection pulse width according to the compensation values from the knock table. The control target is that of restricting the values of KE positions over the $\overline{threshold}$ line. As shown in Figure 4.26, the $\overline{threshold}$ line may be able to assign closer to the $\overline{knock}$ line for increasing the rate of using alternate fuel instead of diesel, but must be avoided for frequently the knock onset. In this case, the $\overline{threshold}$ line is assigned to the middle of separated area between the $\overline{normal}$ line and the $\overline{knock}$ line in order to save the durability of the test engine.

The diagram of the table update method shown in Figure 4.27 can be summarized as: if the mean of five KE values is less than threshold then updating the knock table by decreasing, but if the minimum of five KE values is more than threshold while engine load more than 0%, then updating the knock table by increasing.

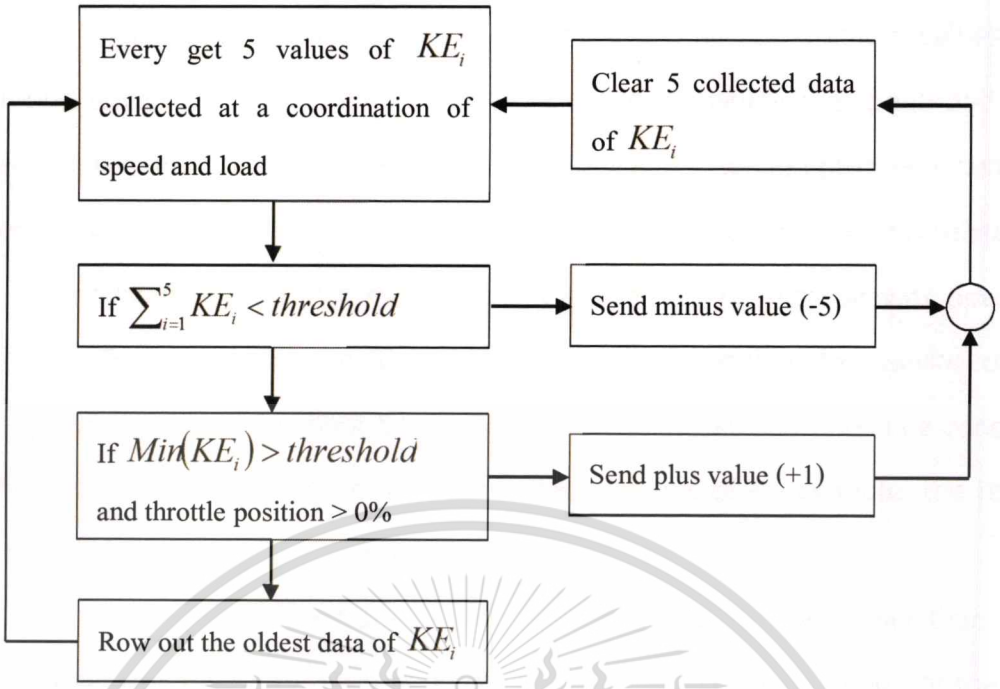

Figure 4.27 Diagram of table update method for knock control

4.3.9 Knock Control Results

Before the experiment of knock control, all of the values in the knock table were set to zero. Figure 4.28 shows an update of knock table which had been processed during the experiment. Each value in the table is referenced by the coordination of the engine speed and load descripted by: x-axis corresponding to the engine speed in RPM and y-axis corresponding to the throttle position (related to engine load) in percentage.

	400	600	800	1000	1200	1400	1600	2000	2500	3000	3500	4000	4500	5000	5500	6000
0	0	-15	-120	-120	-120	-120	-25	-5	0	-5	0	0	0	0	0	0
6	0	-20	-120	-60	-10	-15	-15	0	0	0	0	0	0	0	0	0
12	0	0	-19	-89	44	25	54	27	5	1	0	0	0	0	0	0
18	0	0	-4	-85	50	67	76	62	7	0	0	2	0	0	0	0
24	0	0	3	-119	49	64	41	42	13	2	0	2	0	0	0	0
30	0	0	6	-12	-20	20	17	32	3	8	0	4	0	0	0	0
37	0	0	3	0	-26	1	17	4	10	8	0	6	0	0	0	0
44	0	0	2	8	-10	2	3	1	6	0	0	1	0	0	0	0
51	0	0	2	-2	0	3	12	-9	0	0	0	1	0	0	0	0
58	0	0	0	4	2	-1	2	-1	0	1	0	1	0	0	0	0
65	0	0	0	0	3	0	6	3	0	0	0	0	0	0	0	0
72	0	0	0	0	3	3	7	-12	3	0	0	0	0	0	0	0
79	0	0	0	4	2	3	4	8	2	2	0	0	0	0	0	0
86	0	0	0	0	0	0	0	-16	0	0	0	0	0	0	0	0
93	0	0	0	-9	0	4	2	18	1	2	0	0	0	0	0	0
100	0	0	0	5	0	2	4	4	0	0	0	0	0	0	0	0

Figure 4.28 Knock table updated after the experiment of knock control

In Figure 4.28, the zero values, which mean as the non-updated values, can be found largely over the entire knock table especially where the speed and load exceeding the limit of engine operation. For instance, the section of table where the speed is higher than 4000 RPM can be found only the value of zero and related to the non-updated section. However, in this experiment, the test car was operated under the normal driving condition without the dynamometer, the varying of the specific load and speed cannot be reached to complete all the operating condition in the knock table. Considering to the updated sections of knock table, the results can be subdivided into the following:

1. In the cases of idle speed and deceleration, e.g. speed lower than 1000 RPM or load less than 6%, this section of the table appears with a group of the high negative values.

2. In the cases of power operating condition, such as the speed from 1200 to 3000 RPM and the load between 12%–37%, a group of the positive values is contained in this section of the table.

4.3.9.1 Results of idle speed and deceleration

Figure 4.29 and Figure 4.30 show the results of the knock control experiment that are represented by the KE values (X-mark). The $\overline{normal}$, $\overline{threshold}$ and $\overline{knock}$ lines are obtained by the linear curve fitting from Figure 4.26 with the corresponding speeds of: 756 RPM for Figure 4.29 and 1023 RPM for Figure 4.30.

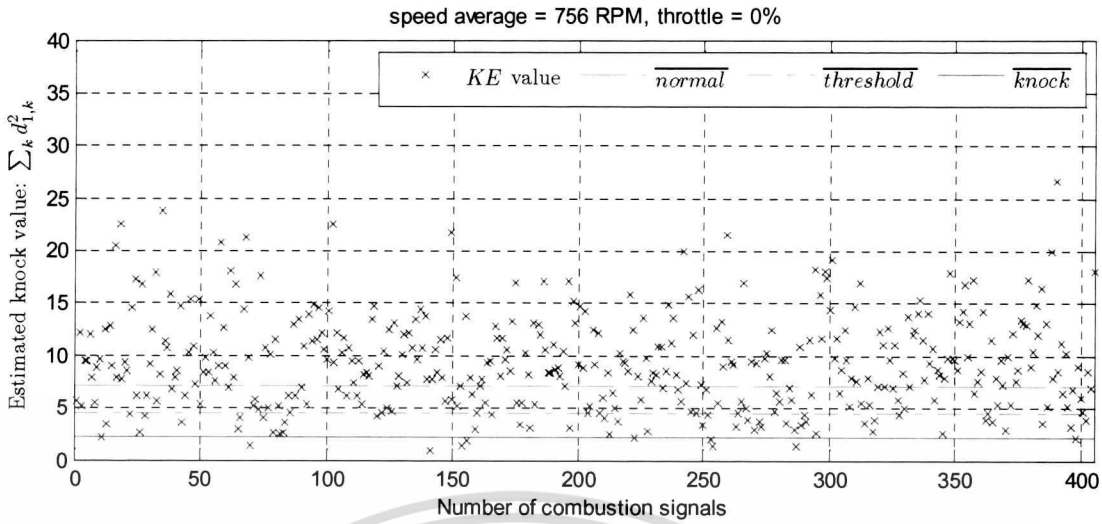

Figure 4.29 Result of knock estimation at the engine speed of 750 RPM

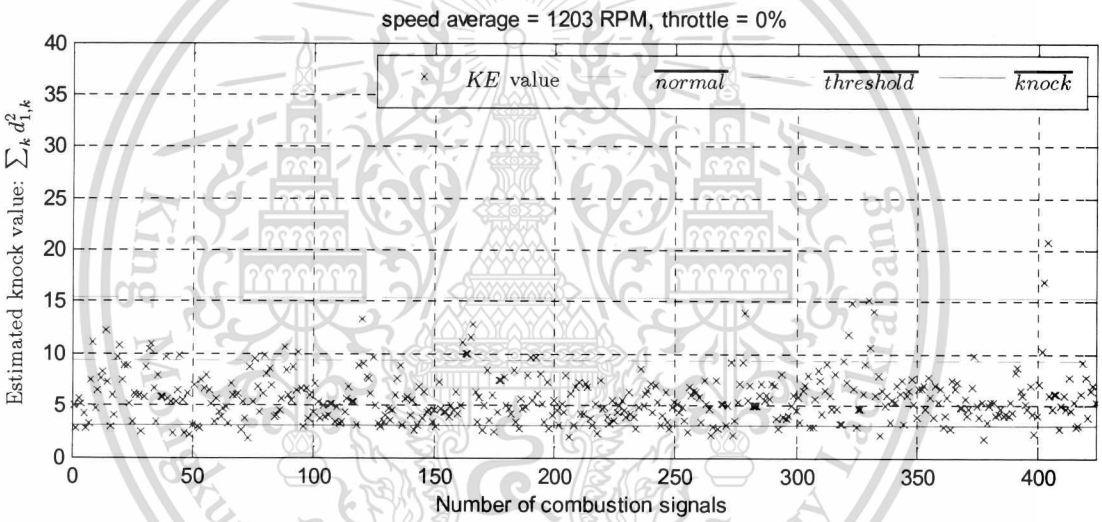

Figure 4.30 Result of knock estimation at the engine speed of 1200 RPM

According to the information of the speed and the percent of throttle position (0%), the case of idle speed can be selected and showed in Figure 4.29. Besides that, the case of during engine deceleration is also showed in Figure 4.30. In both cases, the plots of KE values appear near by the $\overline{knock}$ line but cannot relate to the actual knock combustion. Since the diesel injection control supplies the small amount of diesel fuel to the engine during deceleration and idle operations, the combustion is also reduced accordingly. For this reason, the energy of vibration due to the combustion is about too low represented as KE values in the knock zone. Respect to the fact that any additional fuel does not require for supplement

during deceleration and idle operations, so the injection of alternate fuel should be disabled. Fortunately, the misinterpretation of KE values in the knock zone can benefit to disable the gas injection because the negative values are updated to the knock table. Furthermore, in this case of idle speed and deceleration, the proposed method allows only the negative values to update to the knock table; consequently, the group of high negative values appears in Figure 4.28.

4.3.9.2 Results of the power operational condition

Figure 4.31 and Figure 4.32 show the experimental results under the power and torque operating condition according to the engine speed and load. As referred by the power-torque diagram of the test engine shown in Figure 4.13, the power and torque range begins with the operational speed of 1500 RPM and reaches to the maximum torque at 2000 RPM. The $\overline{normal}$, $\overline{threshold}$ and $\overline{knock}$ lines are obtained as before, from the results of the treatment data sets in Figure 4.26.

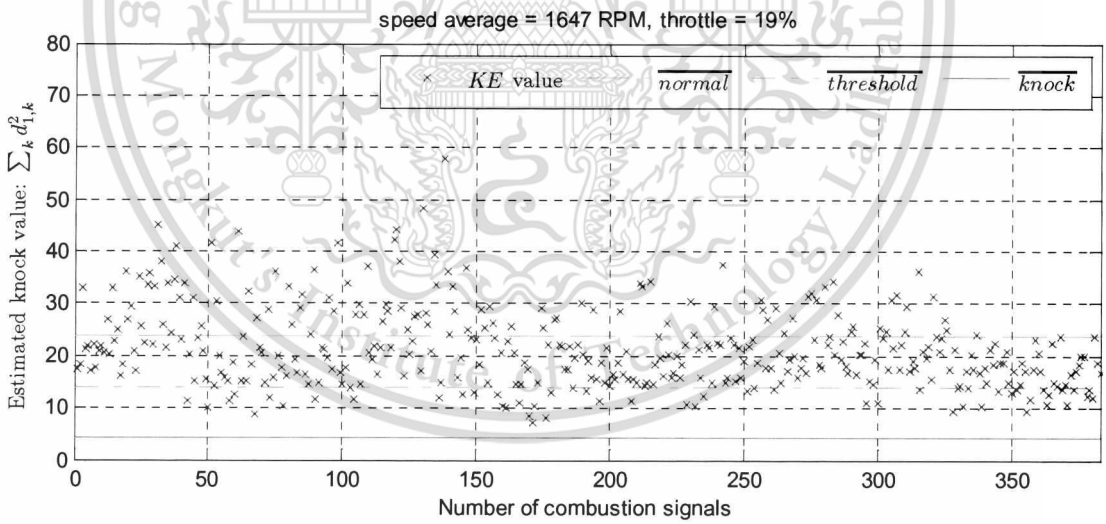

Figure 4.31 Result of knock estimation at the engine speed of 1600 RPM

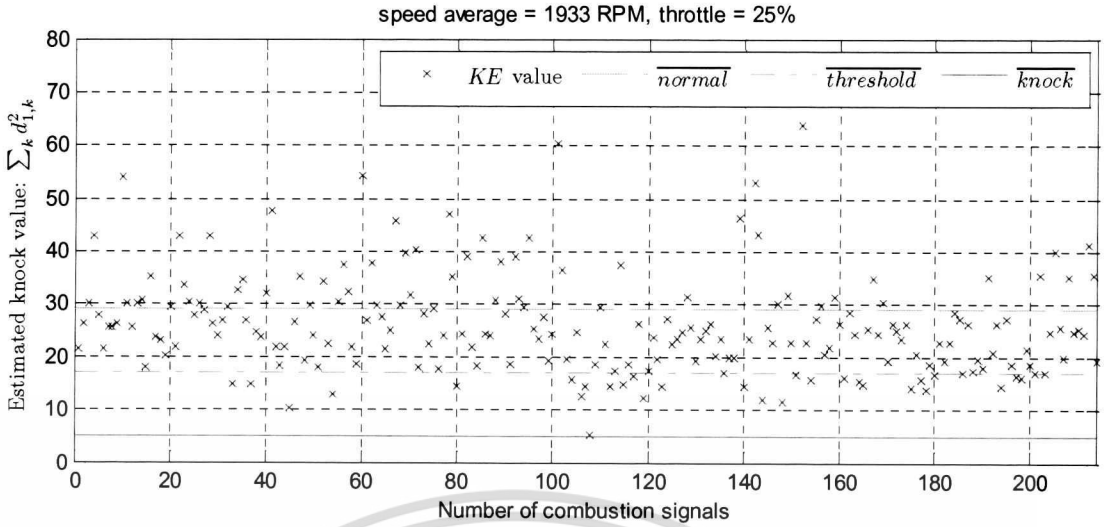

Figure 4.32 Result of knock estimation at the engine speed of 1900 RPM

The results, which are represented by the KE plots, show the same trend from both of the engine speeds around 1600 and 1900 RPM, in Figure 4.31 and Figure 4.32, respectively. Almost all KE values are plotted closely over the $\overline{threshold}$ line. Only a small numbers of them appear below the $\overline{threshold}$ line. Moreover, for more than 550 combustions number in these figures, only 1 point of KE plot can be found in the knock zone. According to the results, the proposed knock control strategy can restrict the KE values to position in the target region over the $\overline{threshold}$ line. The absence of KE values in the knock zone around the $\overline{knock}$ line can be referred to the effective of engine knock elimination.

CHAPTER 5

CONCLUSIONS

This work has been completed on knock control for a diesel dual fuel engine. The new approach knock detection and control strategies are developed based on the experiments. There are three experiments that have been performed in this work, (i) simulation studies, (ii) knock detection and (iii) knock control. The conclusions overall these experiments are summarized as follows:

1. Three knock detection techniques have been explored by the simulation studies, band-pass filter, wavelet-based knock detection and the proposed wavelet-based knock detection with Chi-square, in various ranges of noise level. The comparison results show that the proposed method is the most efficient among all 3 methods. It performs well in all ranges of noise level (i.e. SNR = 0 - 40 dB), whereas the native wavelet-based method can give a good result only in specific SNRs, and the band-pass filter gives the worst result in comparison because it only work in the high SNR only.

2. The proposed wavelet-based knock detection with Chi-square method was also proved in the experiment of knock detection on the real DDF system. According to the experimental results, performing time-frequency filtering and Chi-square thresholding in the wavelet coefficient domain can be able to obtain a precise measure of knock intensity.

3. The experiment of knock control has been completed and proved that the designed knock control method can eliminate the knock phenomena for the traditional DDF system. The experimental results show that almost all knock estimated values not only present in the safety zone but also absent from the knock zone. Accordingly, it also confirms that the controllable intensity of knock in DDF operation is due to the adjustment of alternate fuel injection based on ignition retard control of SI engines. Using the difference in vibration signal during combustion can

be able to predict for the diesel knock onset. Consequently, this scheme can also eventually lead to eliminate the spark knock on account of preventing the heat transfer to the end gas.

Future work should consist of more extensive range of varying engine speed and load as well as operating on a chassis dynamometer. Additional collected data could be analyzed in order to gain a better knock control algorithm for DDF engines. According to this work, the proposed knock control algorithm may also be applied to the auto-calibration technique so as to be a new application of the DDF-ECU. The concept is to start with a small amount of alternative fuel and then gradually increasing while getting the information from a knock sensor for feedback and self-updating to the optimum gas injection in the calibration table.

REFERENCES

[1] Li, Zhen, Zhengjia He, Yanyang Zi, and Hongkai Jiang. **"Rotating machinery fault diagnosis using signal-adapted lifting scheme."** Mechanical Systems and Signal Processing, April 2008: 542-556.

[2] Campos, Marcelo p., and Carlos A. dos Reis Filho. **"Knock sensor signal conditioner."** Proceedings of the 5th IEEE-ICCDCS. Dominican Republic, 2004. 259-263.

[3] Carstens-Behrens, S., and J.F. Bohme. **"Fast knock detection using pattern signals."** Proceedings of IEEE-ICASSP,. Salt Lake City, UT , USA, 2001. 3145-3148.

[4] Cesario, N., F. Taglialatela, and M. Lavorgna. **"SI engine control applications based on in-cylinder pressure signal processing."** Vehicle Power and Propulsion, IEEE Conference. 2005.

[5] Daubechies, I., and W. Sweldens. **Factoring Wavelet Transforms into Lifting Steps.** Vols. 4, No.5, in J. Fourier Anal. Appl., 245-267. 1998.

[6] Drapper, C. S. **"Pressure waves accompanying detonation in the internal combustion engine."** Journal of Aeronautical Sciences 5 (1938): 219-226.

[7] Dunn, Patrick F. **Measurement and Data Analysis for Engineering and Science. International.** McGraw-Hill, 2005.

[8] Fiolka, J. **"A Fast Method For Knock Detection Using Wavelet Transform."** Mixed Design of Integrated Circuits and System. Gdynia, Poland, 2006. 621-626.

[9] Gschweitl, K., E. Gotthard, and A. Kampitsch. **"Real Time Knock Analysis for Automatic Engine Mapping and Calibration."** SAE Technical Paper 942399. 1994.

[10] Intersil Corporation. **"Engine Knock Sensing Applications (HIP9011EVAL1Z)."** Application Note No. AN9770.1. November 6, 2006.

[11] Lin, Jing, and Aimin Zhang. **"Fault feature separation using wavelet-ICA filter."** NDT & E International, September 2005: 421–427.

[12] Mallat, S.G. **"A theory for multiresolution signal decomposition: the wavelet representation."** Pattern Analysis and Machine Intelligence, IEEE Transactions. 1989. 674-693.

REFERENCES (CONT.)

[13] Nakamura, N., E. Ohno, M. Kanamaru, and T Funayama. **"Detection of Higher Frequency Vibration to improve Knock Controllability."** SAE Technical Paper 871912. 1987. 1-8.

[14] NWAFOR, O M I. **Knock characteristics of dual-fuel combustion in diesel engines using natural gas as primary fuel.** Vols. 27, Part 3, in Sadhana, 375–382. 2002.

[15] Ravier, Philippe, and Pierre-Olivier Amblard. **"Wavelet packets and de-noising based on higher-order-statistics for transient detection."** Signal Processing, September 2001: 1909-1926.

[16] Urlaub, M., and J.F. Bohme. **"Evaluation of knock begin in spark ignition engines by least squares."** Proceedings of IEEE-ICASSP. Philadelphia, PA, USA, 2005. v/681-v/684.

[17] Wannatong, K., N. Akarapanyavit, S. Siengsanorh, and S. Chanchaona. **"Combustion and Knock Characteristics of Natural Gas Diesel Dual Fuel Engine."** SAE Technical Paper. 07 23, 2007.

[18] Zhu, Z.K., Ruqiang Yan, Liheng Luo, Z.H. Feng, and F.R. Kong. **"Detection of Signal Transients Based on Wavelet and Statistics for Machine Fault Diagnosis."** Mechanical Systems and Signal Processing, May 2009: 1076-1097.

AUTHOR BIOGRAPHY

Name	Mr. Patin Pongkacha
Date of Birth	September 18, 1981
Place of Birth	Chanthaburi, Thailand
Education	2004 B. Eng. in Electrical Engineering, Kasetsart University
Scholarship	2007–2009 Master Scholarship in Automotive Engineering, Thailand Advanced Institute of Science and Technology and Tokyo Institute of Technology (TAIST-Tokyo Tech)
Knowledge Taxonomy	- Embedded System - Automatic Control - Automotive Electronics
Work Experience	2004–2012 Research Assistant under the Advanced Automation and Electronics Research Unit, National Electronics and Computer Technology Center